

NASA CONTRACTOR  
REPORT

NASA CR-120517

(NASA CR-120517) THERMAL ANALYSIS OF  
M551 EXPERIMENT FOR MATERIALS PROCESSING  
IN SPACE Final Report (Massachusetts  
Inst. of Tech.) 50 p HC \$3.75 CSCL 13H

N75-10966

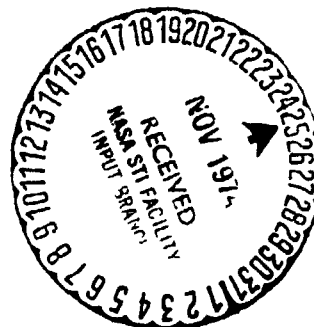
Unclas  
G3/12 53830

THERMAL ANALYSIS OF M551 EXPERIMENT FOR  
MATERIALS PROCESSING IN SPACE

By T. Muraki and K. Masubuchi  
Massachusetts Institute of Technology  
Cambridge, Massachusetts

November 1974

Final Report



Prepared for

NASA-GEORGE C. MARSHALL SPACE FLIGHT CENTER  
Marshall Space Flight Center, Alabama 35812

1. REPORT NO. NASA CR-120517	2. GOVERNMENT ACCESSION NO.	3. RECIPIENT'S CATALOG NO.
4. TITLE AND SUBTITLE THERMAL ANALYSIS OF M551 EXPERIMENT FOR MATERIALS PROCESSING IN SPACE		5. REPORT DATE November 1974
		6. PERFORMING ORGANIZATION CODE
7. AUTHOR(S) T. Muraki and K. Masubuchi		8. PERFORMING ORGANIZATION REPORT #
9. PERFORMING ORGANIZATION NAME AND ADDRESS Massachusetts Institute of Technology Cambridge, Massachusetts		10. WORK UNIT NO.
		11. CONTRACT OR GRANT NO. NAS 8-28732
12. SPONSORING AGENCY NAME AND ADDRESS National Aeronautics and Space Administration Washington, D. C. 20546		13. TYPE OF REPORT & PERIOD COVERED Contractor Report
		14. SPONSORING AGENCY CODE

## 15. SUPPLEMENTARY NOTES

16. ABSTRACT

Heat flow in a disc due to moving heat generated by electron beam was studied analytically.

Computer programs based on the finite-element method were developed for the analysis of two and three dimensional mathematical models.

The limited experimental data were compared with the analytical results and various factors which had influence on heat flow in the disc were studied. Among various factors radiation seemed to be important for the analysis of the disc which was stored in a chamber.

The computer programs were modified to consider the effects of metal melting and solidification as well as of radiation. Temperature dependency of thermo-physical properties was also considered in the program.

17. KEY WORDS		18. DISTRIBUTION STATEMENT Unclassified - Unlimited  <i>W. K. Kludman</i>	
19. SECURITY CLASSIF. (of this report) Unclassified	20. SECURITY CLASSIF. (of this page) Unclassified	21. NO. OF PAGES 49	22. PRICE NTIS

## TABLE OF CONTENTS

	Page
SECTION I. INTRODUCTION.....	1
SECTION II. DEVELOPMENT OF M.I.T. EFFORTS.....	1
A. Phase A: Preparation of the Ground Base Study Plan.....	1
B. Phase B: Laboratory Test Plan.....	2
C. Phase C: Experiment Analysis Program.....	3
SECTION III. DEVELOPMENT OF ANALYSIS.....	3
A. Sample Specimen.....	4
B. Predicted Experimental Conditions...	4
C. Two-Dimensional Analysis.....	5
1. Two-Dimensional Model.....	5
2. Analytical Results.....	6
3. Discussion.....	6
D. Three-Dimensional Analysis.....	6
1. Three-Dimensional Model.....	6
2. Analytical Results.....	7
3. Discussion.....	8
E. Experimental Data and Analysis.....	8
F. Computer Program.....	9
G. Conclusion.....	9
SECTION IV. APPENDICES.....	10
Appendix A.....	10
Appendix B.....	11
Appendix C.....	12
Appendix D.....	19
Appendix E.....	20
SECTION V. REFERENCES.....	21

PRECEDING PAGE BLANK NOT FILMED

## LIST OF ILLUSTRATIONS

Figure	Title	Page
1.	Mesh Pattern and Node Arrangement for Finite Element Analysis of Disc.....	22
2.	Calculated Temperature Histories of Nodes on Weld Circle in Quadrant 1.....	23
3.	Calculated Temperature Histories of Nodes on Weld Circle in Quadrant 2.....	24
4.	Calculated Temperature Histories of Nodes on Weld Circle in Quadrant 3.....	25
5.	Calculated Temperature Histories of Nodes on Weld Circle in Quadrant 4.....	26
6.	Calculated Temperature Histories of Nodes inside of Weld Circle in Quadrant 1.....	27
7.	Calculated Temperature Histories of Nodes inside of Weld Circle in Quadrant 2.....	28
8.	Calculated Temperature Histories of Nodes inside of Weld Circle in Quadrant 3.....	29
9.	Mesh Pattern and Node Arrangement for Finite Element Analysis of Disc.....	30
10.	Calculated Temperature Histories of Points on Weld Circle in Quadrant 1.....	31
11.	Calculated Temperature Histories of Points on Weld Circle in Quadrant 2.....	32
12.	Calculated Temperature Histories of Points on Weld Circle in Quadrant 3.....	33
13.	Calculated Temperature Histories at Point where Heat Source Dwells.....	34
14.	Calculated Temperature Histories of Nodes outside of Weld Circle in Quadrant 1.....	35

Figure	Title	Page
15.	Calculated Temperature Histories of Nodes outside of Weld Circle in Quadrant 2.....	36
16.	Calculated Temperature Histories of Nodes outside of Weld Circle in Quadrant 3.....	37
17.	Calculated Temperature Histories of Nodes concerning Dwelling Heat Source.....	38
18.	Analytical and Experimental Temperature Histories of Point in Quadrant 1.....	39
19.	Analytical and Experimental Temperature Histories of Point in Quadrant 2.....	40
20.	Analytical and Experimental Temperature Histories of Point in Quadrant 3.....	41
A-1.	Finite Elements Prepared for Analysis.....	42
A-2.	Basic Three-Dimensional Element and Nodal Names.....	43
A-3.	Models to Consider Metal Melting.....	44

## SUMMARY

Heat flow in a disc due to moving heat generated by electron beam was studied analytically.

Computer programs based on the finite-element method were developed for the analysis of two- and three-dimensional mathematical models.

The limited experimental data were compared with the analytical results and various factors which had influence on heat flow in the disc were studied. Among various factors radiation seemed to be important for the analysis of the disc which was stored in a chamber.

The computer programs were modified to consider the effects of metal melting and solidification as well as of radiation. Temperature dependency of thermophysical properties was also considered in the program.

## SECTION I: INTRODUCTION

The objective of the M551 experiment is to examine the molten flow and solidification of metal alloys during electron-beam melting in space. The specimens are circular discs of Stainless steel, 2219 Aluminum and Tantalum, respectively.

Of the various factors which had an effect on the metal melting and solidification in the experiment, gravity appears to have had the most significant effect, especially in space. However, gravity has no effect on heat conduction and radiation.

The M.I.T. efforts placed emphasis on the heat flow analysis due to conduction and radiation. The information obtained by thermal analysis was intended to assist other contractors in their study on the metal melting and solidification. Mathematical models based on the finite element method were developed to analyze various heat-transfer phenomena involved in the M551 experiment. The computer program by use of the mathematical models was also developed to conduct heat flow analysis of a test specimen which had complex configurations and experimental conditions.

Through the M551 experiment the M.I.T. efforts have been made in the following phases:

- Phase A: Preparation of ground base study plan
- Phase B: Laboratory test program
- Phase C: Experiment analysis program

Phases A and B were completed in 2½ and 12 months, respectively, from the date of contract award. Phase C will be completed in 19 months.

## SECTION II: DEVELOPMENT OF M.I.T. EFFORTS

During Phases A, B and C the M.I.T. efforts basically followed the plan described in the proposal dated April 13, 1972 (Reference 1). The emphasis of the M.I.T. efforts was generally placed on the analytical study.

Phases A, B and C are described as follows:

### A. PHASE A: PREPARATION OF THE GROUND BASE STUDY PLAN

The efforts during Phase A covered the following steps:

Step 1: Collect currently available reports pertinent to this research

Step 2: Consider all possible variables involved in the proposed research

Step 3: Conduct rough, preliminary analysis

Step 4: Evaluate current experimental programs

Step 5: Suggest modification of the current experimental programs

Step 6: Develop detailed plans of suggested experiment

Step 7: Develop detailed plans of analytical research

Efforts also were made to exchange information with researchers in other organizations assigned to studies other than thermal analysis.

#### B. PHASE B: LABORATORY TEST PROGRAM

Phase B was to conduct the study program defined in Phase A. Most of the M.I.T. efforts in Phase B were addressed to the heat flow analysis of the M551 experiment.

A limited thermal analysis was also conducted by Teledyne Brown Engineering previously (Reference 2). The analysis used a finite difference computer program originally developed by Chrysler Corporation. After that, other comprehensive thermal analyses were conducted by M.I.T. (References 3 and 4). Mathematical models based on the finite-element method were developed and applied to analyze the non-stationary heat flow of sample problems. Computers were used extensively in the analysis.

The M.I.T. efforts in Phase B basically consist of the following steps:

Step 8: Develop preliminary model

Step 9: Improve analytical model

Step 10: Analyze data obtained in ground base experiment

In Step 8, a two-dimensional finite-element model was developed. The heat source was assumed to be concentrated at a point, to be distributed evenly along the thickness direction, and to move along a circle at a constant speed. This analysis was expected to give



sufficiently accurate information about heat flow in most regions of the disc except the immediate vicinity of the heat source because the temperature distribution in regions apart from the heat source was presumably two-dimensional. However the temperature distribution in regions near the heat source was predicted to be three-dimensional and the actual heat source was not concentrated at a point but distributed over some region of the disc surface. Therefore Step 9 was to develop a three-dimensional model and analyze the sample problem by use of the combination of the three-dimensional and two-dimensional models.

The combination of those models yielded better information on heat flow in the vicinity of the heat source.

Data obtained in a ground base experiment which was conducted by M.S.F.C. was sent to M.I.T., which was informed that the experiment was carried out under almost the same conditions as those described in Teledyne Brown Engineering's report (See Reference 2). The results obtained by the two-dimensional analysis did not show good agreement with the experimental results. As anticipated, the combination of two-dimensional and three-dimensional models showed the improvement of the analytical results, which were verified by the experimental results.

#### C. PHASE C: EXPERIMENT ANALYSIS PROGRAM

In experiments which have been conducted in space so far, a plan to obtain data on heat flow has not been included. Therefore the efforts during the remainder of Phase B and also Phase C have been addressed to improve the analysis and to study more details of the temperature distribution in regions near the heat source.

Development of the analysis is presented in the following chapter.

### SECTION III: DEVELOPMENT OF ANALYSIS

For the heat flow analysis of the M551 experiment, two types of mathematical models were basically developed: two-dimensional and three-dimensional models.

At the beginning of Phase B, the two-dimensional model based on the finite element method was developed and applied to the heat flow analysis of the disc. Then, considering the varying thickness of the disc and the characteristics of experimental conditions, the three-dimensional model was developed. The model was combined with the two-dimensional model and used to obtain more reasonable results in the vicinity of a heat source.

In the following sections one of the typical sample specimens of the M551 experiment and its analytical results are described.

#### A. SAMPLE SPECIMEN

For the M551 experiment three types of materials were prepared. Their thicknesses were all different. The emphasis of M.I.T. analysis was placed on one of the materials--Stainless steel. The sample specimen used for the analysis is described as follows:

1. It is a circular disc of 6.5 inches in diameter.
2. It consists of four quadrants with different thicknesses of 0.020, 0.050, 0.125, and 0.250 inches.
3. It has a back-up plate which shares the same shaft with it.
4. It is stored in a chamber with other parts such as the back-up plate and a motor housing.

The following values of the 321 Stainless steel are adopted as thermophysical properties of the specimen:

Thermal conductivity	= 12.9 Btu/hr/ft/ <sup>°</sup> F
Specific heat	= 0.14 Btu/lb/ <sup>°</sup> F
Density	= 494 lb/ft <sup>3</sup>
Melting point	= 2600 <sup>°</sup> F
Latent heat of fusion	= 117 Btu/lb

The first three properties are the average values of the 321 stainless steel for the temperature range of interest.

#### B. PREDICTED EXPERIMENTAL CONDITIONS

Experimental conditions were assumed for the analysis as follows:

1. A constant heat is generated by electron beam with 20 kilovolts and 80 milliamperes.\*
2. The efficiency of the electron beam is 80%.
3. The electron beam diameter is 0.125 inch.
4. The disc is heated along a 4.5-inch diameter circle.
5. The disc rotates clockwise with the relative velocity of 37 inches per minute against the electron beam through three quadrants and then dwells for 30 seconds at the middle point on the weld circle in the 0.25-inch thick quadrant.

\* From results of the ground-base experiment, 50 milliamperes were adopted in the analysis which used the combination of two- and three-dimensional elements.

### C. TWO-DIMENSIONAL ANALYSIS

1. Two-dimensional Model. Figure 1 shows a mesh pattern and a node arrangement for the finite-element analysis of a disc. The model consists of two-dimensional finite elements. It contains 232 elements and 216 nodes.

In this analysis the following assumptions were adopted:

- a. Temperature is uniform in the thickness direction.
- b. Thermophysical properties are invariant with temperature.
- c. The radiation between the disc and the surrounding parts is neglected.
- d. The effect of solidification is neglected.
- e. The initial temperature of the disc is uniform at 0°F.\*
- f. The heat source is concentrated at a point and moves along the weld circle.
- g. The effect of the metal melting on heat flow is taken into account by adjusting the intensity of the heat source.

The following melting regions and intensities of heat source are assumed from results of the preliminary analysis.

In Quadrant 1:

1. The assumed melting region----a band with a 0.475-inch width along the weld circle.
2. The applied heating rate----1.017 Btu/sec.

In Quadrant 2:

1. The assumed melting region----a band with a 0.125-inch width along the weld circle.
2. The applied heating rate----1.084 Btu/sec.

In Quadrant 3:

1. Melting does not occur except at Node 113 in Figure 1.
2. The applied heating rate----1.213 Btu/sec.

\* Basically, this assumption is permissible because the linear analysis is adopted. In other words, the temperature, which starts from the initial temperature except zero, is obtained just by adding the initial temperature to the temperature calculated.

In Quadrant 4:

1. The assumed melting region----a circle of 0.125-inch diameter (the size of the electron beam).
2. The applied heating rate----1.110 Btu/sec (during a period when the region goes on melting)----1.213 Btu/sec (during the rest of the above period).

2. Analytical Results. Analytical results of the sample disc are presented in Figures 2 to 8. In those figures numbers on temperature history curves correspond with nodal names in Figure 1. The following results are shown in the figures:

- a. The temperature histories at points on the weld circle of 4.5-inch diameter in Quadrants 1 to 3 (Figures 2 to 4)
- b. The temperature histories at the point where the electron beam dwells and at two other points in Quadrant 4 (Figure 5)
- c. The temperature histories of nodes located inside of the weld circle in Quadrants 1 to 3 (Figures 6 to 8)

From those results the following items are pointed out:

- a. The melting occurs along the weld circle in Quadrants 1 and 2.
- b. At the point where the electron beam dwells, the melting begins about 4 seconds after heat is supplied there.
- c. The melting does not occur at points which are 0.325 inch apart from the weld circle.
- d. The maximum temperature obtained by the two-dimensional model exceeds 10,000°F in Quadrant 1.

3. Discussion. The following discussions are probably made on the results described above:

- a. A point heat source assumed for the analysis is not realistic.
- b. Three-dimensional analysis should be applied to the region near the heat source in Quadrants 3 and 4.
- c. Heat radiation should be considered in the analysis.

#### D. THREE-DIMENSIONAL ANALYSIS

1. Three-dimensional Model. Three-dimensional finite elements were developed to idealize the disc as a three-dimensional model. In practice, the combination of two- and three-dimensional elements

were used to represent a mathematical model of the sample disc. The three-dimensional element was used for the region near the heat source and the two-dimensional element for the rest of the above region.

A mesh pattern and typical nodal names used are shown in Figure 9. The model contains 448 nodes and 336 elements.

In the analysis the following assumptions are adopted:

a. Temperature in the thickness direction is three-dimensional in the region of a band of a 0.5-inch width along the weld circle through Quadrants 2 to 4.

b. In the rest of the above region temperature is uniform in the thickness direction.

c. Thermophysical properties are invariant with temperature.\*

d. The heat exchange due to the radiation between the disc and the surroundings is not considered.\*

e. The effect of metal melting and solidification is not considered.

f. The initial temperature of the disc is uniform at 78°F.

g. The heat source is uniformly distributed over the region of 0.125-inch width band on the upper surface of the disc.

2. Analytical Results. Results obtained by the three-dimensional analysis are shown in Figures 10 to 13. Temperature history curves in the figures denote the average of the temperatures at the nodes shown in the parentheses.

The following results are shown in the figures:

a. The temperature histories at points on the weld circle in Quadrants 1 to 3 (Figures 10 to 12)

b. The temperature histories at the point where the electron beam dwells and at two other points in Quadrant 4 (Figure 13)

c. The temperature histories of nodes located outside of the weld circle in Quadrants 1 to 3 (Figures 14 to 17)

d. The temperature histories in the thickness direction in Quadrants 1 to 3 (Figures 12, 13, 16, and 17)

The following items are observed from the figures:

a. The temperature difference between the upper and the lower surfaces of the disc disappears in a few seconds after the heat source passes over.

\* The computer program is available for the analysis considering these effects.

- b. The melting occurs along the weld circle in Quadrant 1 and at the point where the heat source dwells in Quadrant 4.
- c. The maximum temperature obtained is about 4,500°F in Quadrant 1.

### 3. Discussion.

- a. It is enough to use three-dimensional finite elements to a limited region close to the heat source in Quadrants 3 and 4.
- b. Even in the region in Quadrant 3 mentioned above, temperature becomes uniform in the thickness direction of the disc in a few seconds after the heat source passes over.
- c. The temperature difference of the points close to the heat source in Quadrant 4 keeps almost constant value while heat is supplied.
- d. The heat radiation should be considered in the analysis as the next step because of considering the effect of the surroundings of the disc.

## E. EXPERIMENTAL DATA AND ANALYSIS

Data obtained by a ground-base experiment was sent to M.I.T. by Lockheed. It was informed that the experiment was basically conducted in the same conditions that were used in the Teledyne Brown Engineering's report (Reference 2).

Generally speaking, the experimental results did not show good agreement with the analytical ones, as expected. This will probably come from two reasons, one of which is that details of the experimental conditions are not confirmed. The other reason is that factors neglected or simplified in the analysis have influence, which is not predictable, on the analytical results.

Under the circumstances three nodes close to the weld circle are chosen to compare the experimental results with the analytical results.

Figure 18 shows the temperature history of a point in Quadrant 1.

The experimental result is different from the analytical one. The difference is possibly caused by the differences between the heat intensities supplied in the experiment and those assumed for the analysis. In addition, the effect of melting on the heat flow of the disc will not be negligible because the thickness of the disc is very thin in this quadrant. The velocity of the electron beam is slower than that adopted in the analysis.

Figures 19 and 20 show the temperature histories of typical points in Quadrants 2 and 3, respectively. In those figures, the correlation between the experimental and the analytical results seems to be reasonable. However the heat actually supplied to the disc is presumably more than that used in the analysis. The effect of the heat radiation is also observed from Figures 19 and 20.

## F. COMPUTER PROGRAM

Computer programs based on the finite element method were developed for the analysis of non-stationary heat transfer problems. Among various programs two programs were mainly used to analyze heat flow of the specimen. One is for the two-dimensional analysis and another for the three-dimensional analysis. In the three-dimensional analysis program a two-dimensional finite element as well as a three-dimensional one are prepared to idealize the specimen as the combination of the two types of element.

The following guidelines were considered in developing the computer programs.

1. The program can be applied to a heat flow analysis of any two- or three-dimensional body.
2. Both specified temperature and supplied heat are treated as boundary conditions.
3. The effect of radiation can be considered.
4. Metal melting and solidification can be considered.
5. Non-stationary heat flow problem as well as stationary one can be solved by the same program.
6. Thermophysical properties are allowed to depend on temperature.
7. The program should be flexible for future improvement or modification.

These items have been achieved so far. Details and manuals of the programs will be presented later.

## G. CONCLUSION

The heat flow analysis of the M551 experiment was conducted at M.I.T. In the analysis, only the disc was considered. In other words, the surroundings of the disc were ignored. The computer programs based on the finite-element method were developed for the analysis.

The disc was idealized as the two-dimensional mathematical model at first. Then the three-dimensional model was developed, which consisted of the combination of two- and three-dimensional finite elements.

The analytical results obtained by the three-dimensional model were compared with the limited experimental data. From the comparison it became clear that the heat radiation had influence on the heat flow of the problem in consideration.

The computer programs are now available for the analysis considering the radiation. The programs also cover the effect of metal melting and solidification and the temperature dependency of thermophysical properties.

## SECTION IV: APPENDICES

### APPENDIX A

#### Symbols

$A$	Area
$C$	Heat Capacity
$K$	Absolute temperature
$k_x, k_y, k_z$	Thermal conductivity
$n_x, n_y, n_z$	Components of unit normal vector
$\dot{Q}$	Rate of internal heat generation
$T$	Temperature
$\bar{T}$	Prescribed temperature
$T_M$	Melting point
$t$	Time
$V$	Volume
$x, y, z$	Position coordinates
$\epsilon$	Emissivity
$\lambda_f$	Latent heat of fusion
$\rho$	Density
$\sigma$	Stefan-Boltzmann Constant



## APPENDIX B

Generally speaking, the finite element method is based on the principle of virtual work or the principle of complementary virtual work. They are dual principles.

In this report, the principle of virtual work is applied to the analysis of a non-stationary heat transfer problem. This principle is widely applied to analyze problems in various fields because the existence of potential function is not required.

For the analysis of the M551 experiment, both two- and three-dimensional models were developed by use of the finite element method. Emphasis of the formulation is placed on the three-dimensional model in the following section.

The governing equation and the corresponding boundary conditions are given for the three-dimensional heat transfer problem as follows:

$$\frac{\partial}{\partial x} \left( k_x \frac{\partial T}{\partial x} \right) + \frac{\partial}{\partial y} \left( k_y \frac{\partial T}{\partial y} \right) + \frac{\partial}{\partial z} \left( k_z \frac{\partial T}{\partial z} \right) + \dot{Q} = c\rho \frac{\partial T}{\partial t} \quad \text{in } V \quad (A-1)$$

$$T = \bar{T} \quad \text{on } A_2 \quad (A-2)$$

$$n_x k_x \frac{\partial T}{\partial x} + n_y k_y \frac{\partial T}{\partial y} + n_z k_z \frac{\partial T}{\partial z} + \epsilon \sigma (K^4 - K_o^4) = 0 \quad \text{on } A_3 \quad (A-3)$$

where  $A_2$  denotes the surface on which temperature is specified and  $A_3$  the surface from which heat emission due to radiation occurs. Equation (A-3) presents the Stefan-Boltzmann law modified for a grey body. The principle of virtual work which is equivalent to equations (A-1) and (A-3) is obtained as follows:

$$\begin{aligned} & \iiint_V \left\{ k_x \frac{\partial T}{\partial x} \delta \left( \frac{\partial T}{\partial x} \right) + k_y \frac{\partial T}{\partial y} \delta \left( \frac{\partial T}{\partial y} \right) + k_z \frac{\partial T}{\partial z} \delta \left( \frac{\partial T}{\partial z} \right) + c\rho \frac{\partial T}{\partial t} \delta T \right\} dV \\ & + \iint_{A_2} \epsilon \sigma (K^4 - K_o^4) \delta T dA - \iiint_V \dot{Q} \delta T dV = 0 \end{aligned} \quad (A-4)$$

In equation (A-4), temperature must satisfy equation (A-2) on boundary  $A_2$ . In other words, equation (A-2) is the subsidiary condition for equation (A-4).

In addition, it is noticed here that terms concerning time such as  $\frac{\partial T}{\partial t}$  and  $\dot{Q}$  are assumed to be constant during variation  $\delta T$  in derivation of equation (A-4).

## APPENDIX C

### Finite Element Approach

In formulating a non-stationary heat transfer problem, the concept of finite element is adopted for the space coordinate and that of finite difference for the time coordinate.

As seen in equation (A-4), this equation leads to the nonlinear one. To solve the equation, an iterative procedure is commonly used. However, if that procedure is applied to a transient problem such as the non-stationary heat transfer problem, computing time for the analysis will increase tremendously. In order to avoid this disadvantage and also to keep the simplicity of the finite element method in its formulation, temperature which determines the emission of radiation energy from a body is assumed to be known. In other words, the emission is assumed to be obtained by using the temperature at the latest time step which is known. This assumption will be valid if the temperature change during one time step is small. Under the above assumption, the formulation of the problem by use of the finite element method becomes straightforward.

As shown in Figure A-1, the two-dimensional and three-dimensional elements are used together to analyze the heat conduction problem of the disc. However, three-dimensional analysis is mainly described here.

In the finite element analysis, a body of interest is imaginarily divided into a finite number of elements. Therefore, equation (A-4) is written as follows:

$$\begin{aligned} & \sum_{i=1}^N \iiint_{V_i} \left\{ k_x \frac{\partial T}{\partial x} \delta \left( \frac{\partial T}{\partial x} \right) + k_y \frac{\partial T}{\partial y} \delta \left( \frac{\partial T}{\partial y} \right) + k_z \frac{\partial T}{\partial z} \delta \left( \frac{\partial T}{\partial z} \right) \right. \\ & \quad \left. + c \rho \frac{\partial T}{\partial t} \delta T \right\} dV + \sum_{i=1}^{N_2} \iint_{A_{2_i}} \epsilon \sigma (K^4 - K_o^4) \delta T dA \\ & - \sum_{i=1}^N \iiint_{V_i} Q \delta T dV = 0 \end{aligned} \quad (A-5)$$

where  $N$  and  $N_2$  are total number of elements and that of areas concerning radiation, respectively.

For a typical three-dimensional element shown in Figure A-2, temperature distribution in it is to be assumed by the following polynomials.

$$T = \alpha_0 + \alpha_1 x + \alpha_2 y + \alpha_3 z \quad (A-6)$$

This is also written in the matrix form as follows.

$$T = [1, x, y, z] \begin{Bmatrix} \alpha_0 \\ \alpha_1 \\ \alpha_2 \\ \alpha_3 \end{Bmatrix} \quad (A-7)$$

Equation (A-7) is further written concisely

$$T = [A]\{\alpha\} \quad (A-8)$$

where

$$[A] = [1, x, y, z] \quad (A-9.1)$$

$$\{\alpha\}^T = [\alpha_0, \alpha_1, \alpha_2, \alpha_3] \quad (A-9.2)$$

As seen from Figure A-2,  $\{\alpha\}$  is related with the temperatures at the nodes of an element as follows.

$$\begin{Bmatrix} T_1 \\ T_2 \\ T_3 \\ T_4 \end{Bmatrix} = \begin{bmatrix} 1 & x_1 & y_1 & z_1 \\ 1 & x_2 & y_2 & z_2 \\ 1 & x_3 & y_3 & z_3 \\ 1 & x_4 & y_4 & z_4 \end{bmatrix} \begin{Bmatrix} \alpha_0 \\ \alpha_1 \\ \alpha_2 \\ \alpha_3 \end{Bmatrix} \quad (A-10)$$

where  $x_1, y_1, \dots$ , and  $z_4$  denote the coordinates of the corresponding nodes.

For simplicity, equation (A-10) is written as follows.

$$\{T\} = [N]\{\alpha\} \quad (A-11)$$

where

$$\{T\}^T = [T_1, T_2, T_3, T_4] \quad (A-12.1)$$

$$[N] = \begin{bmatrix} 1 & x_1 & y_1 & z_1 \\ 1 & x_2 & y_2 & z_2 \\ 1 & x_3 & y_3 & z_3 \\ 1 & x_4 & y_4 & z_4 \end{bmatrix} \quad (A-12.2)$$

Substituting equation (A-11) into equation (A-8), the assumed temperature distribution in an element is represented in the following form.

$$T = [A][N]^{-1}\{T\} \quad (A-13)$$

By using equation (A-13), each integral term in equation (A-5) is easily written in terms of nodal temperature.

Differentiating equation (A-13), the following expression is obtained.

$$\begin{pmatrix} \frac{\partial T}{\partial x} \\ \frac{\partial T}{\partial y} \\ \frac{\partial T}{\partial z} \end{pmatrix} = [B][N]^{-1}\{T\} \quad (A-14)$$

where

$$[B] = \begin{bmatrix} 0 & 1 & 0 & 0 \\ 0 & 0 & 1 & 0 \\ 0 & 0 & 0 & 1 \end{bmatrix} \quad (A-15)$$

Using equation (A-14), the first three terms in equation (A-5) are written as follows.

$$\delta\{T\}^T ([N]^{-1})^T \iiint_{V_1} [B]^T [K] [B] dV [N]^{-1} \{T\} \quad (A-16)$$

where

$$[K] = \begin{bmatrix} k_x & 0 & 0 \\ 0 & k_y & 0 \\ 0 & 0 & k_z \end{bmatrix} \quad (A-17)$$

Similarly, the fourth term is written as follows.

$$\delta\{T\}^T ([N]^{-1})^T \iiint C_p [A]^T [A] dV [N]^{-1} \{T\} \quad (A-18)$$

where

$$\dot{\{T\}}^T = \left[ \frac{\partial T_1}{\partial t}, \frac{\partial T_2}{\partial t}, \frac{\partial T_3}{\partial t}, \frac{\partial T_4}{\partial t} \right] \quad (A-19)$$

The fifth term in equation (A-5) reminds us of the assumption mentioned above. Under the assumption that the absolute temperature on the boundary  $A_{2_1}$  is known, that the term is represented as

follows.

$$\delta\{T\}^T ([N]^{-1})^T \iint_{A_{2_1}} [A]^T \epsilon \sigma (K^4 - K_o^4) dA \quad (A-20)$$

The last term is written in a similar form to that of equation (A-20).

$$\delta\{T\}^T ([N]^{-1})^T \iiint_{V_1} [A]^T Q dv \quad (A-21)$$

For the expressions (A-16), (A-18), (A-20) and (A-21), the following matrices and vectors are defined.

$$[H] = ([N]^{-1})^T \iiint_{V_1} [B]^T [K] [B] dv [N]^{-1} \quad (A-22)$$

$$[P] = ([N]^{-1})^T \iiint_{V_1} c \rho [A]^T [A] dv [N]^{-1} \quad (A-23)$$

$$\{F_R\} = ([N]^{-1})^T \iint_{A_{2_1}} [A]^T \epsilon \sigma (K^4 - K_o^4) dA \quad (A-24)$$

$$\{F_Q\} = ([N]^{-1})^T \iiint_{V_1} [A]^T Q dv \quad (A-25)$$

Using the expressions (A-22) to (A-25), equation (A-5) is written as follows.

$$\begin{aligned} \sum_{i=1}^N \delta\{T\}^T [H] \{T\} + \sum_{i=1}^N \delta\{T\}^T [P] \{T\} + \sum_{i=1}^{N_2} \delta\{T\}^T \{F_R\} \\ - \sum_{i=1}^N \delta\{T\}^T \{F_Q\} = 0 \end{aligned} \quad (A-26)$$

The summation symbol in the above equation denotes that components in a matrix or vector concerning each element are entered in their position of the global matrix or vector. For simplicity, the same symbols as those for an element are adopted to represent the characteristic matrices and vectors for a whole body. Then, equation (A-26) is written as follows.

$$\delta\{T\}^T [H]\{T\} + \delta\{T\}^T [P]\{\dot{T}\} + \delta\{T\}^T \{F_R\} - \delta\{T\}^T \{F_Q\} = 0 \quad (A-27)$$

In equation (A-27),  $\delta\{T\}$  is arbitrary. Therefore, the following equation is obtained so that equation (A-27) is held.

$$[H]\{T\} + [P]\{\dot{T}\} - \{F\} = \{0\} \quad (A-28)$$

where

$$\{F\} = \{F_Q\} - \{F_R\} \quad (A-29)$$

To the time coordinate, a finite difference method is usually applied. In this report, the following finite difference scheme is used.

$$\{T\}_i = \{T\}_{i-1} + \frac{\Delta t}{2} (\{\dot{T}\}_i + \{\dot{T}\}_{i-1}) \quad (A-30)$$

where subscripts  $i$  and  $i-1$  denote time,  $t_i$ , and  $t_{i-1}$ , respectively;  $\Delta t$  is the time interval between  $t_i$  and  $t_{i-1}$ . Using equation (A-30), equation (A-28) is transformed as follows.

$$([H] + \frac{2}{\Delta t} [P])\Delta\{T\}_i = -2[H]\{T\}_{i-1} + \{F\}_{i-1} + \{F\}_i \quad (A-31)$$

where

$$\Delta\{T\}_i = \{T\}_i - \{T\}_{i-1}$$

(A-32)

Therefore, if the initial condition is given, equation (A-31) can be solved step-by-step at every time increment.



## APPENDIX D

### Finite Element Models

Concerning the heat conduction analysis of the disc, several types of finite element were used, as shown in Figure A-1. Two of them are two-dimensional models and others are three-dimensional models. Both of the two- and three-dimensional models contain a composite element. These composite elements are introduced in order to make it easy to generate data input for the analysis and also to improve the accuracy of the solution.

As seen from Figure A-1, the two-dimensional composite element consists of the average of four triangular elements and the three-dimensional element, the average of ten tetrahedra. In addition, these composite elements as well as a simple triangular element or a simple tetrahedron assure the continuity of the assumed temperature distribution on the boundary between adjacent elements. This continuity condition is required so that the solution of equation (A-5) approaches the exact solution when the number of elements increases.

## APPENDIX E

### A Basic Concept to Consider Metal Melting and Solidification

In the finite-element analysis of heat conduction problems, it is possible to consider metal melting and solidification. For example, metal melting is considered in the analysis as follows. The problem is to estimate how much heat is spent for metal melting and what is the temperature of an element of interest.

First, consider an element with the volume of  $dV$ . Then, suppose the average temperature of the element is  $T$ , at time  $t$  and  $T$  is below the melting point of the metal. If the temperature increases during the next time increment, we may expect one of the cases as shown in Figure A-3.

In Case a), the average temperature of the element is still below the melting point. Therefore, the same procedure as before will be taken for the following calculation.

In Case b), the average temperature is beyond the melting point and heat storage during the time increment is enough to melt the element completely. Therefore, we have the following relation.

$$q_T = q_1 + q_M + q_2 \quad (A-33)$$

where  $q_T$  and  $q_M$  denote heat stored in the element and heat spent to melt the element, respectively.  $q_1$  and  $q_2$  are represented as follows.

$$q_1 = Cp (T_M - T_1) dV \Delta t \quad (A-34.1)$$

$$q_2 = Cp (T_2 - T_M) dV \Delta t \quad (A-34.2)$$

In equation (A-33),  $q_T$  is calculated from the temperature,  $T_2'$ , which is the original one obtained at time,  $t_2$ , as follows

$$q_T = Cp(T_2' - T_1) dV \Delta t \quad (A-35)$$

Using the latent heat of fusion,  $\lambda_f$ ,  $q_M$  is obtained as follows

$$q_M = dV \lambda_f \quad (A-36)$$

Therefore, substituting equations (A-34) to (A-36) into equation (A-33), the modified temperature,  $T_2$ , at the time  $t_2$  can be calculated. For the next calculation, the temperature  $T_2$  is treated as the initial condition.

In Case c), the average temperature of the element of interest is also beyond the melting point, but heat storage during the given time increment is not enough to melt the whole element. Therefore, the following relation is obtained instead of equation (A-33)

$$q_T = q_1 + q_M \quad (A-37)$$

$q_T$  and  $q_1$  are given in the same form as equations (A-35) and (A-34.1), respectively. On the other hand,  $q_M$  is given as follows.

$$q_M = dV' \lambda_f \quad (A-38)$$

where  $dV' < dV$  which means that the whole element of interest does not melt. For the next calculation, the melting point  $T_M$  is treated as the initial condition.

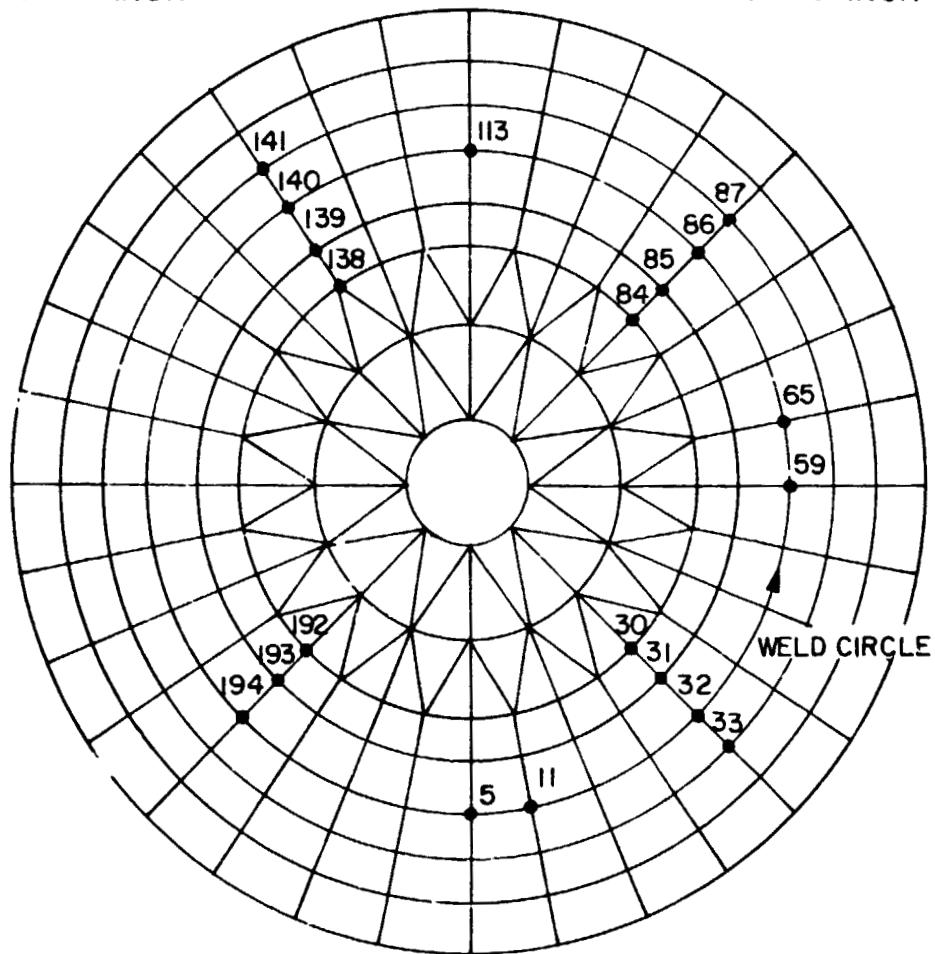
In the case of solidification, the procedure considered in the computer program is the same as that for melting, except that the temperature decreases.

## SECTION V: REFERENCES

1. M.I.T.: Proposal in Response to Request No. 8-1-2-65-28009 on Thermal Analysis of M551 through M554 Experiments for Materials Processing in Space to G.M.S.F.C. April 13, 1972.
2. Teledyne Brown Engineering: Thermal Analysis of Low-g Stainless Steel Welding Experiment. Technical Letter ASD-AS1N-14159, March 23, 1972.
3. Muraki, T. and Masubuchi, K.: First Interim Report on Phase B of Thermal Analysis of M551 Experiment for Materials Processing in Space. NASA-MSFC Contractor Report, January 15, 1973.
4. Muraki, T. and Masubuchi, K.: Phase B of Thermal Analysis of M551 Experiment for Materials Processing in Space. NASA-MSFC Contractor Report, July 18, 1973.

QUADRANT 3  
0.125 INCH

QUADRANT 2  
0.050 INCH



QUADRANT 4  
0.250 INCH

QUADRANT 1  
0.020 INCH

DISK : 6.5 INCH  $\phi$   
WELD CIRCLE : 4.5 INCH  $\phi$

Figure 1 Mesh Pattern and Node Arrangement for Finite Element Analysis of Disc

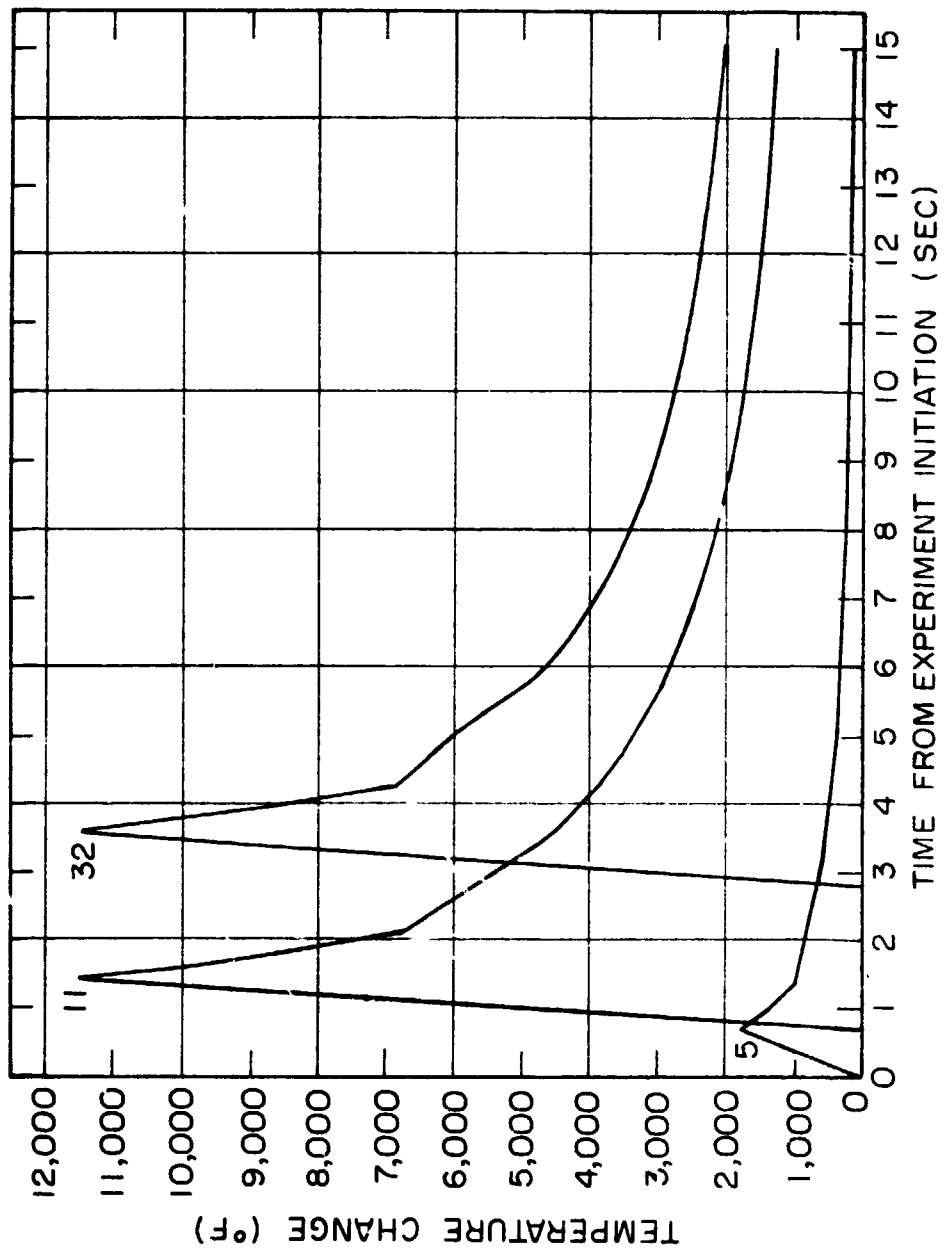


Figure 2 Calculated Temperature History of Nodes on Weld Circle in Quadrant 1

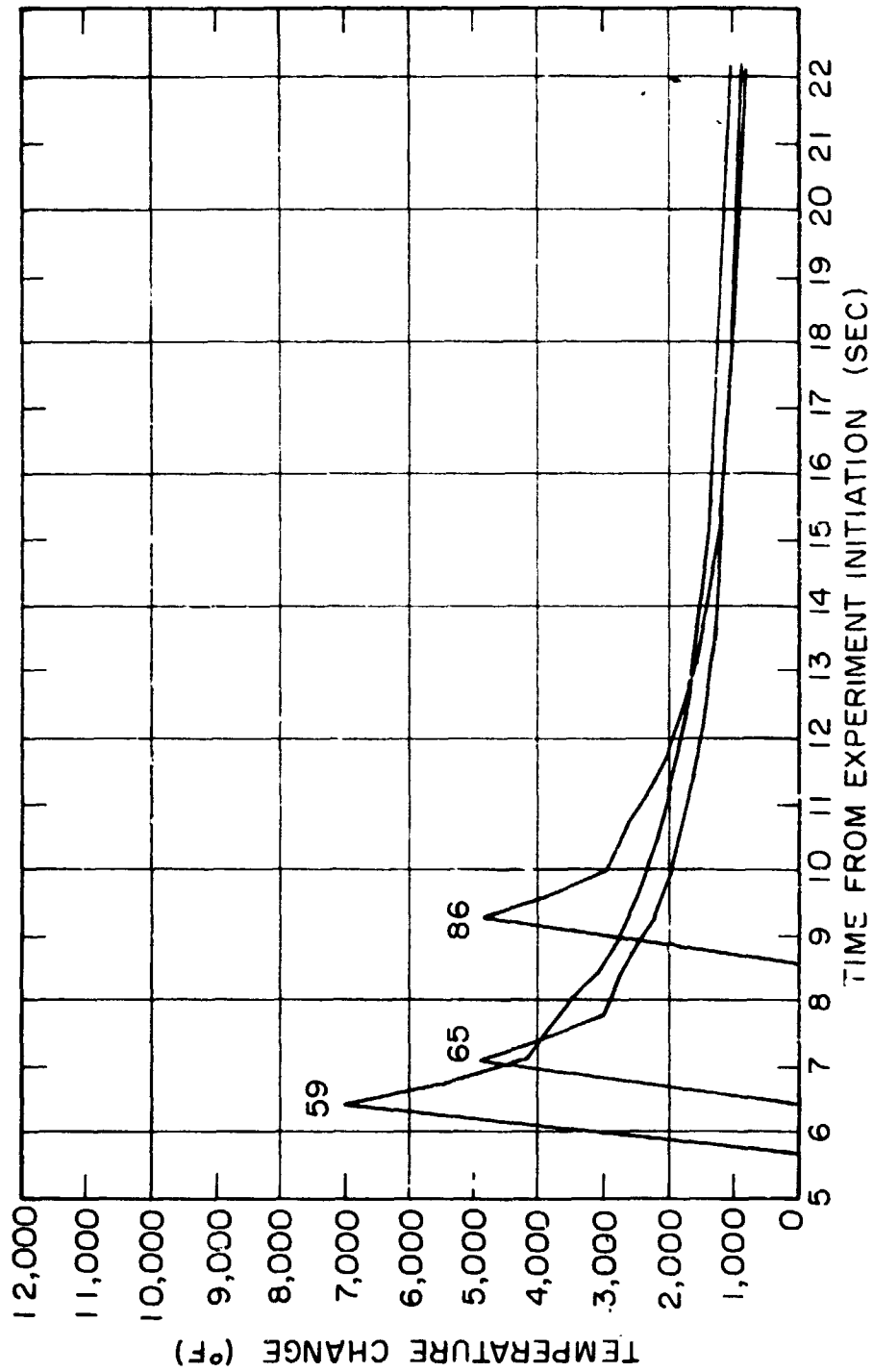


Figure 3 Calculated Temperature Histories of Nodes on Weld Circle in Quadrant 2

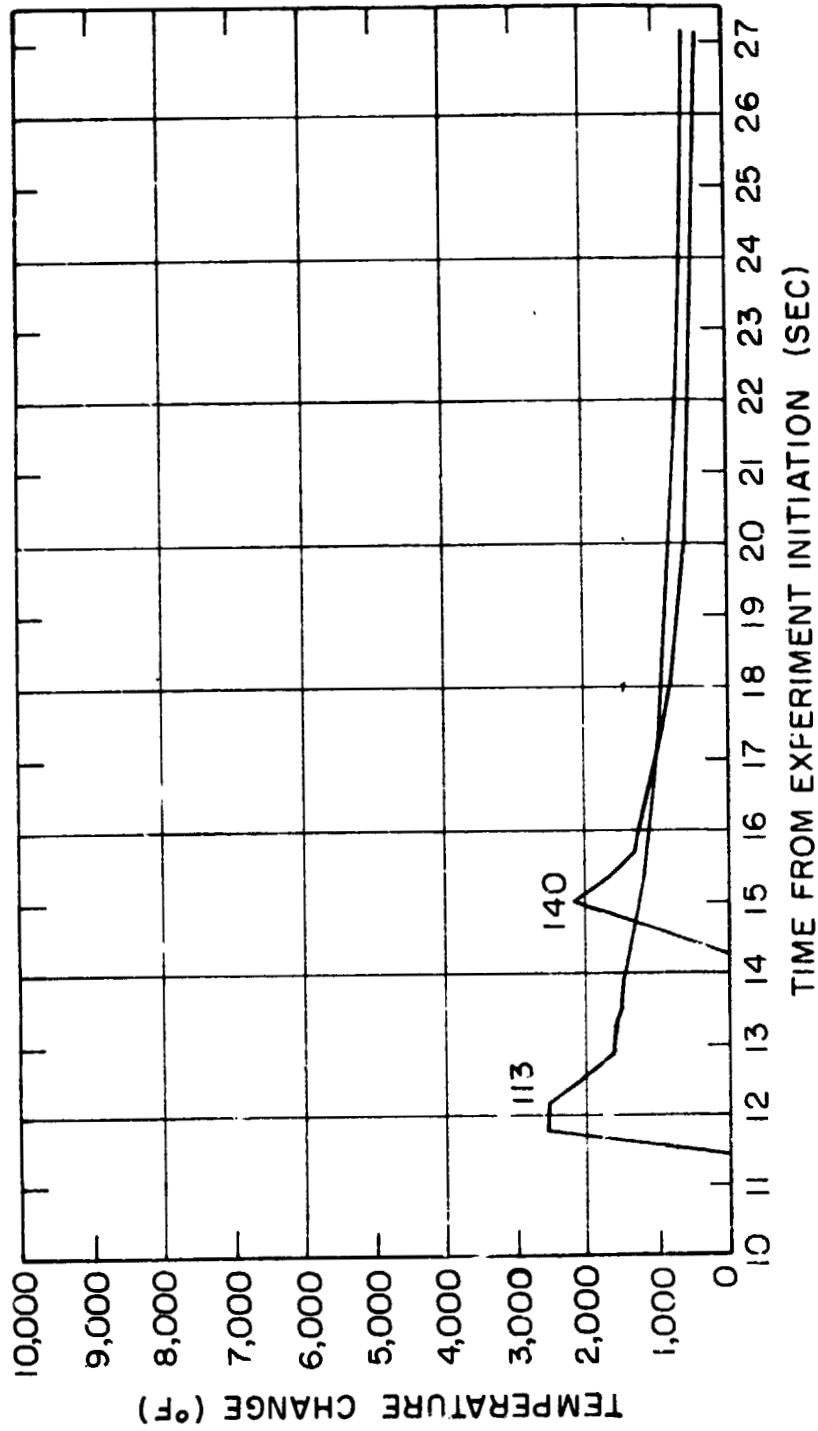


Figure 4 Calculated Temperature Histories of Nodes on Weld Circle in Quadrant 3

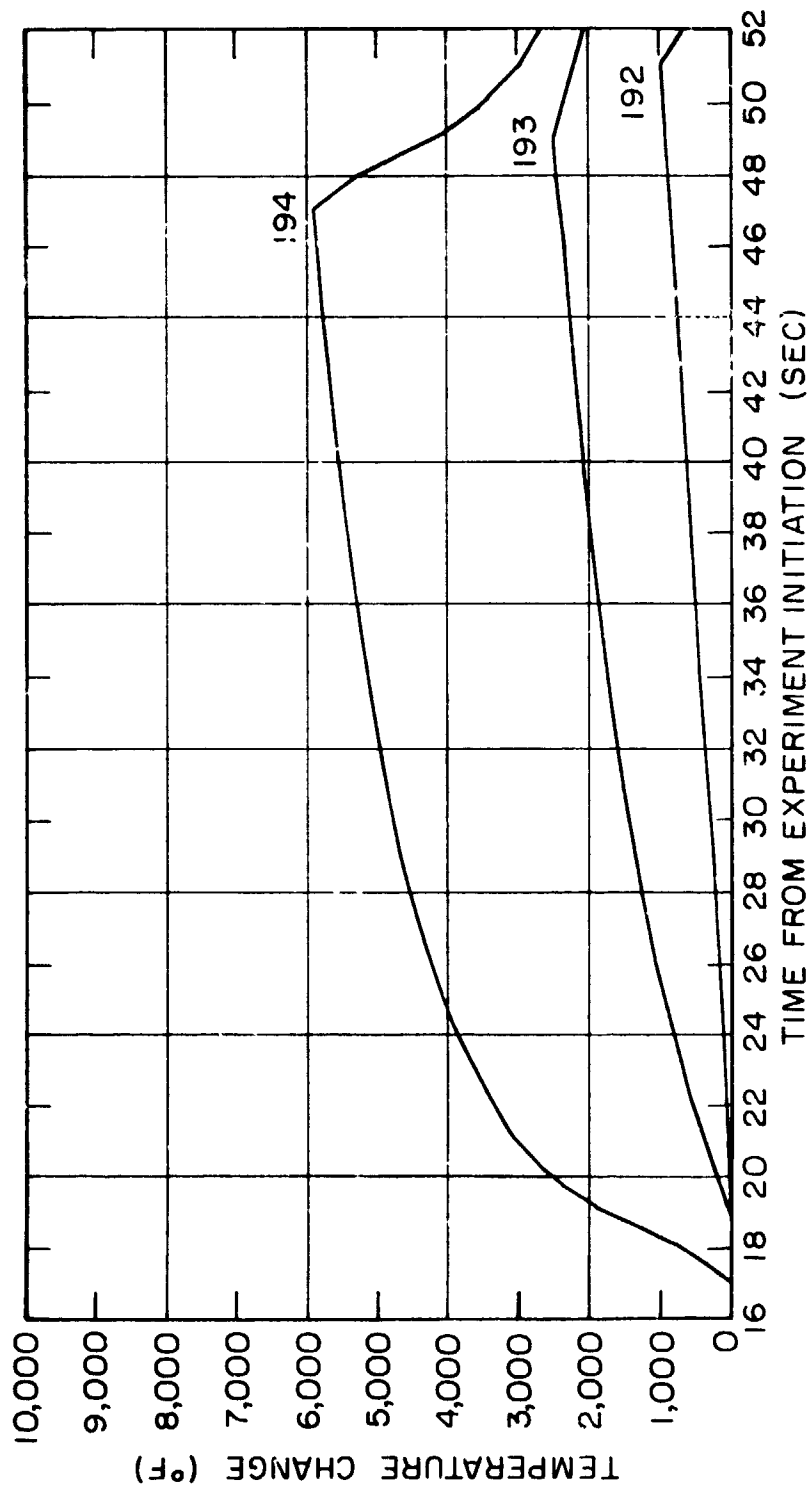


Figure 5 Calculated Temperature Histories 1f Nodes on Weld Circle in Quadrant 4



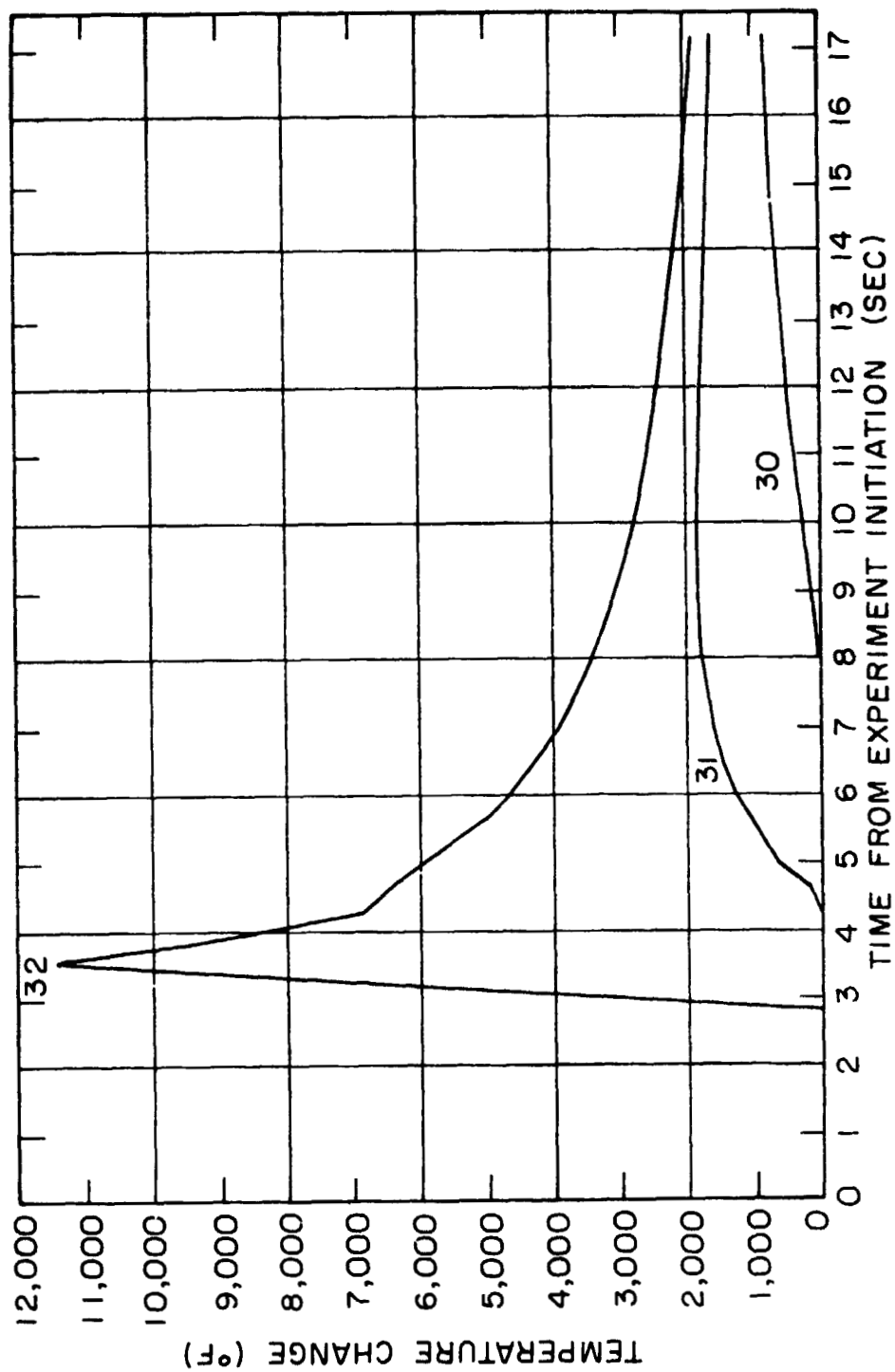


Figure 6 Calculated Temperature Histories of Nodes inside of Weld Circle in Quadrant 1

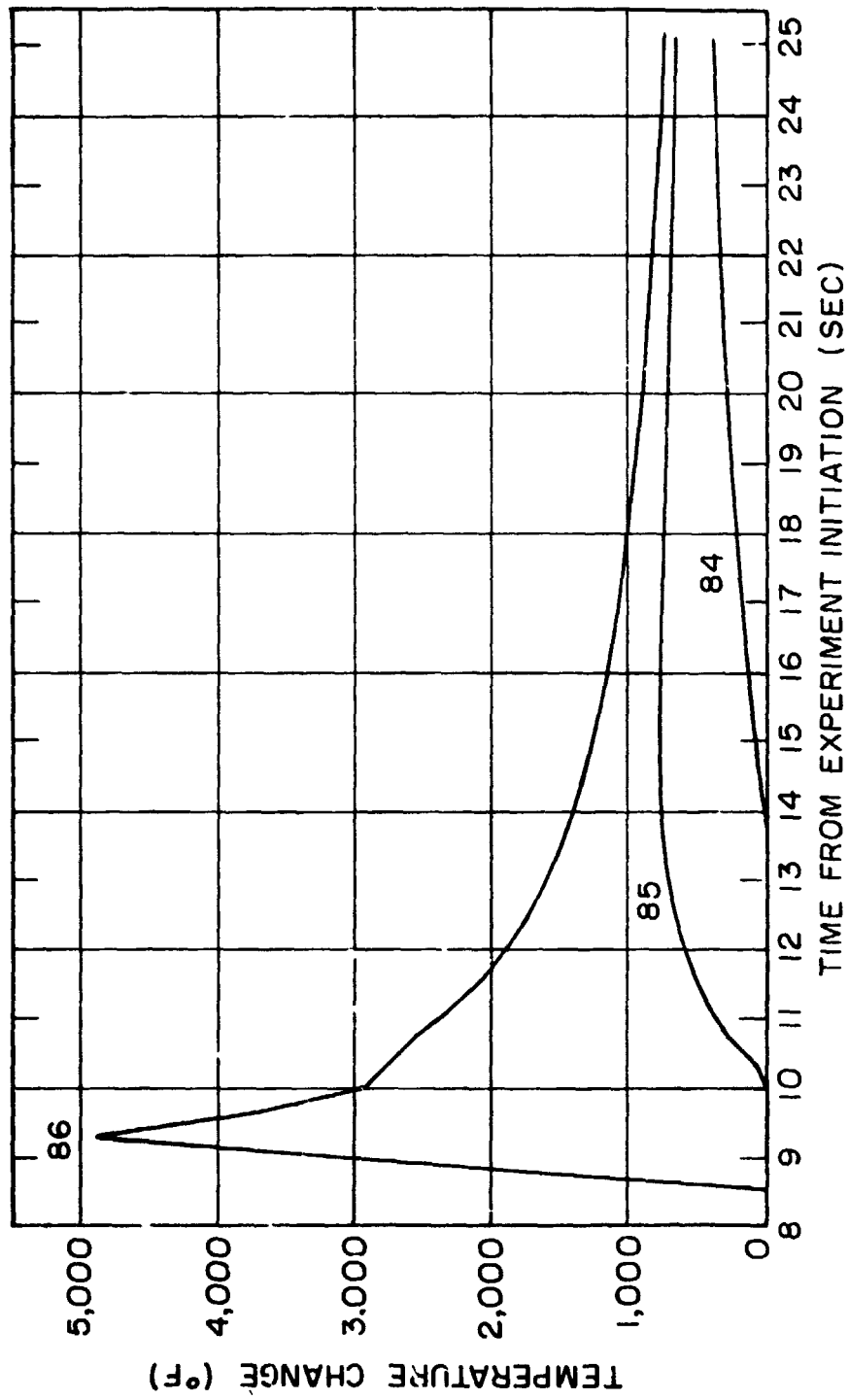


Figure 7 Calculated Temperature Histories of Nodes inside of Weld Circle in Quadrant 2

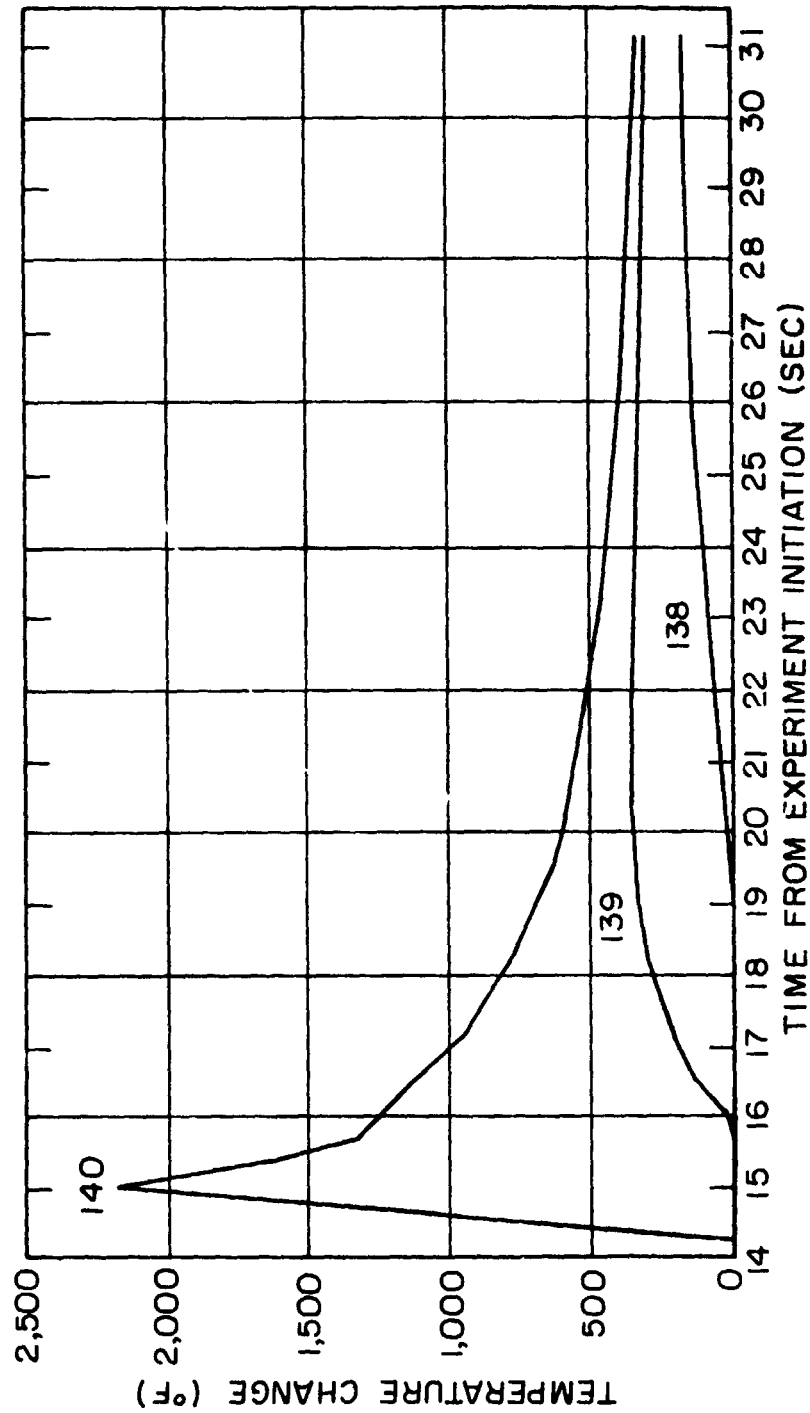
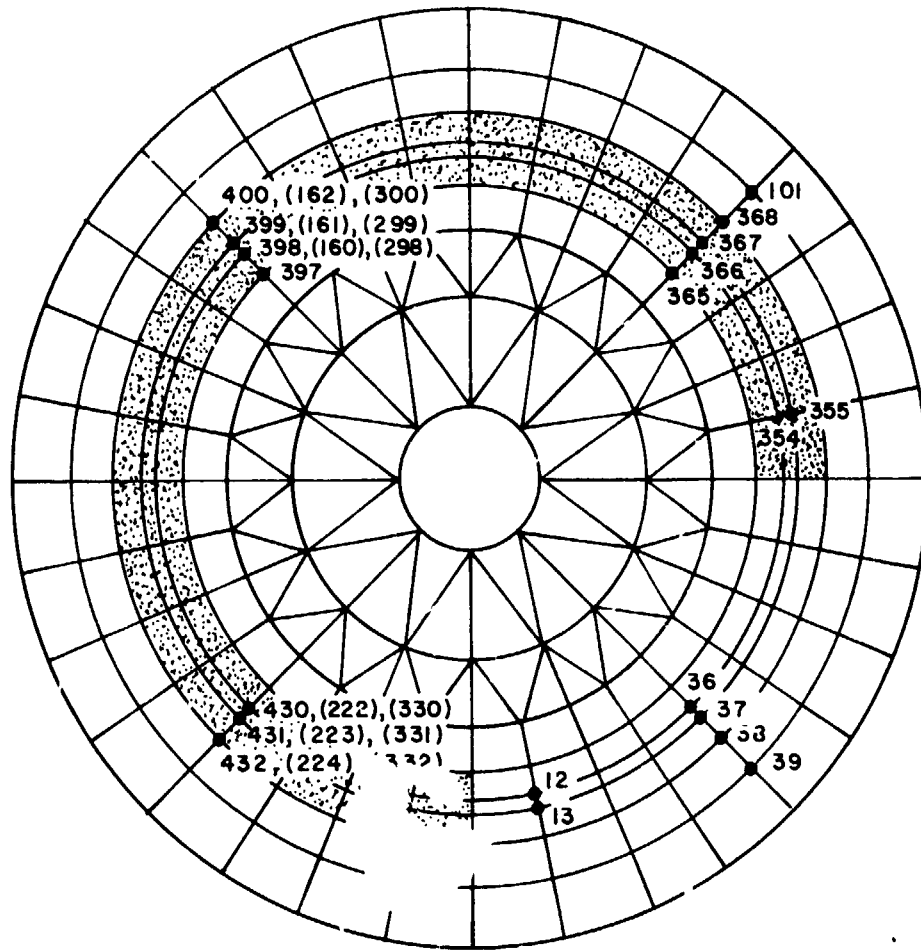


Figure 8 Calculated Temperature Histories of Nodes inside of Weld Circle in Quadrant 3

QUADRANT 3  
0.125 INCH

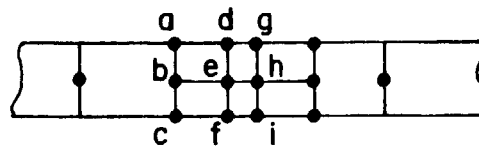
QUADRANT 2  
0.050 INCH



QUADRANT 4  
0.250 INCH

QUADRANT 1  
0.020 INCH

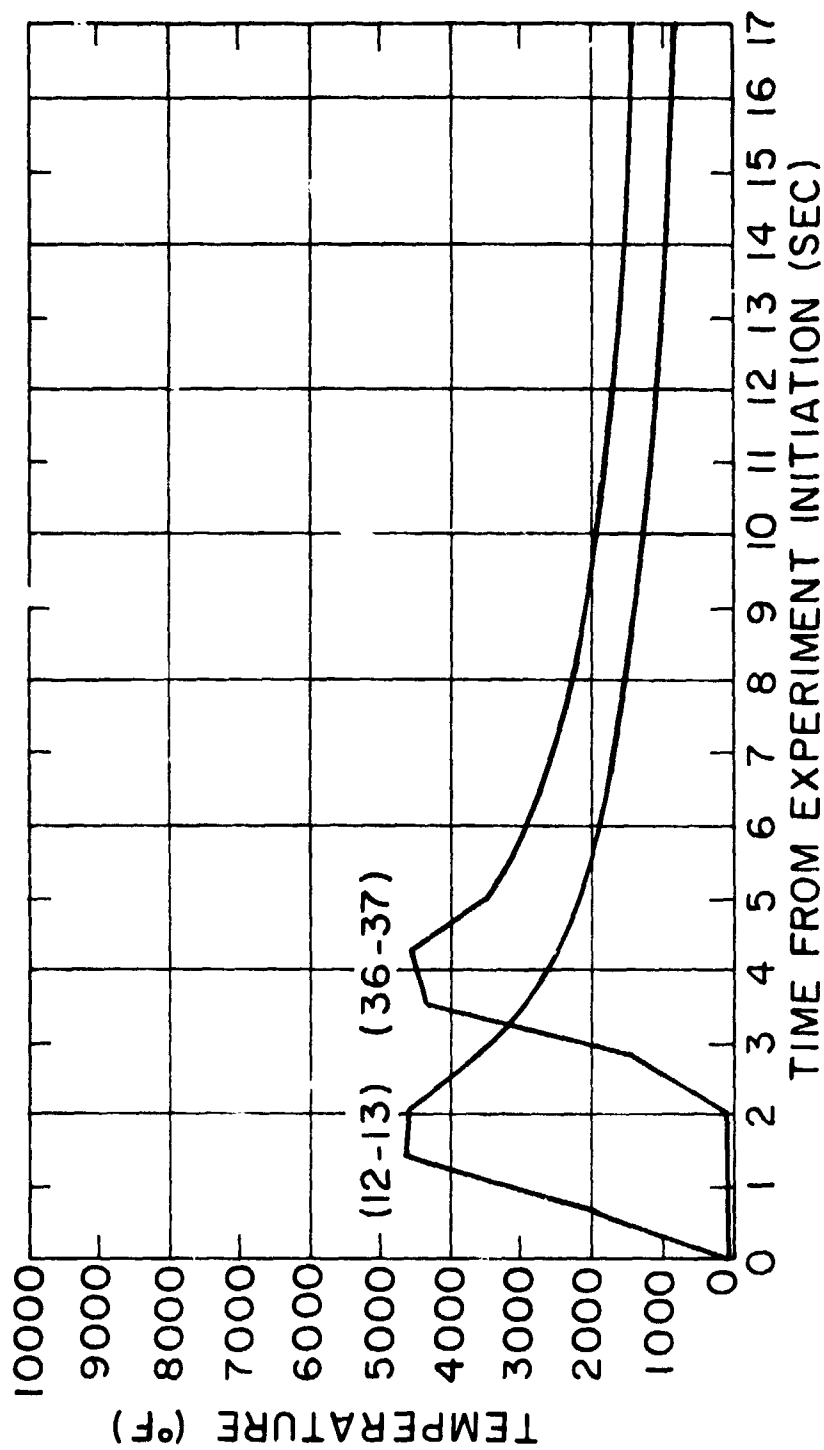
a = 432  
b = 224  
c = 332



d = 431    g = 430  
e = 223    h = 222  
f = 331    i = 330

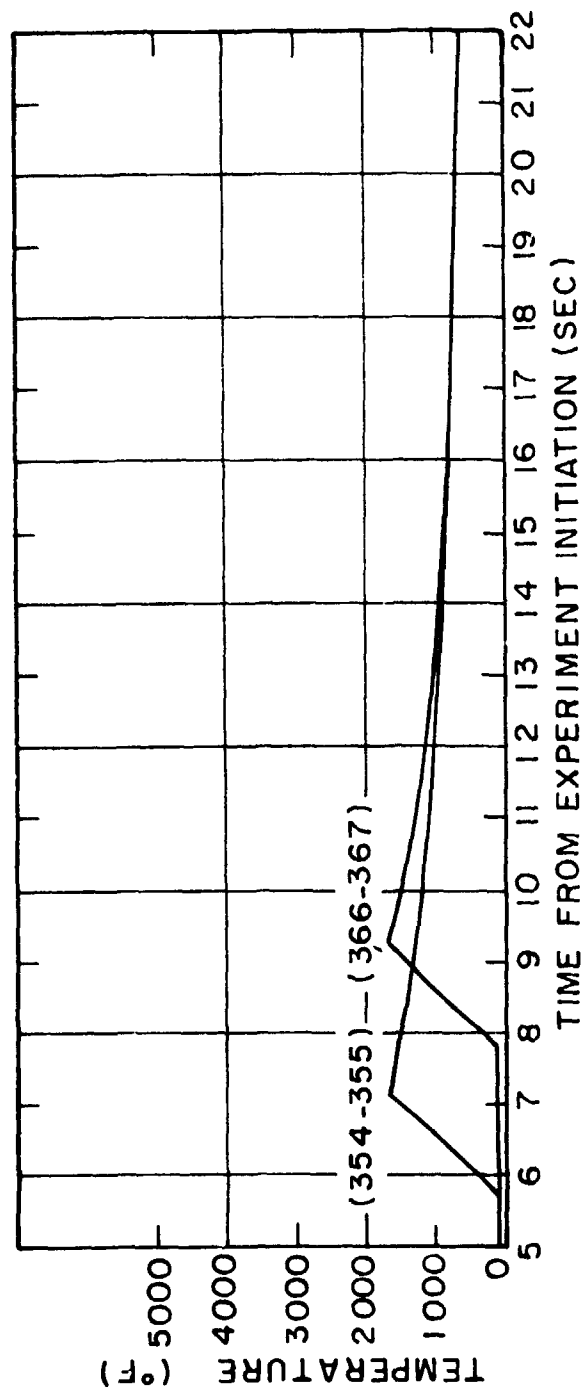
Note: Dotted portions consist of three-dimensional elements.  
Numbers in parentheses denote subsurfaces and an example is shown in the above enlarged figure of a section in Quadrant 4.

FIGURE 9 Mesh Pattern and Node Arrangement  
for Finite Element Analysis of Disc



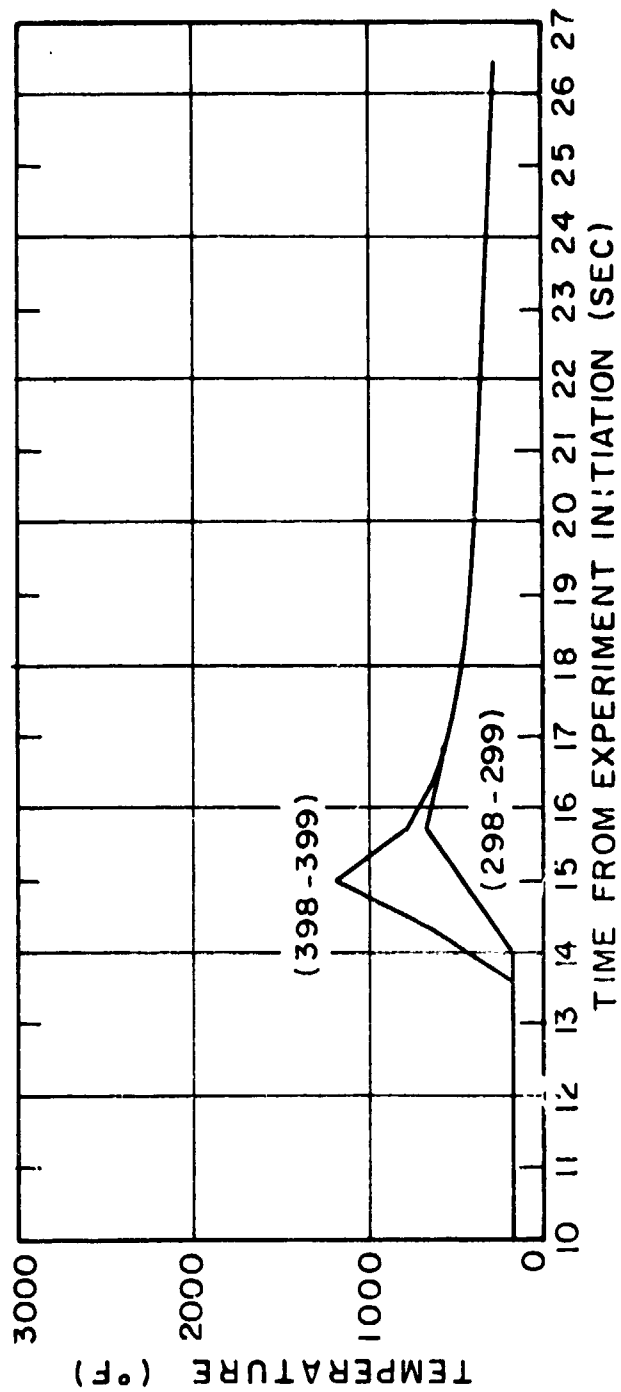
Note: Curves denote the average temperatures of nodes in the parentheses

Figure 10 Calculated Temperature Histories of Points on Weld Circle in Quadrant 1



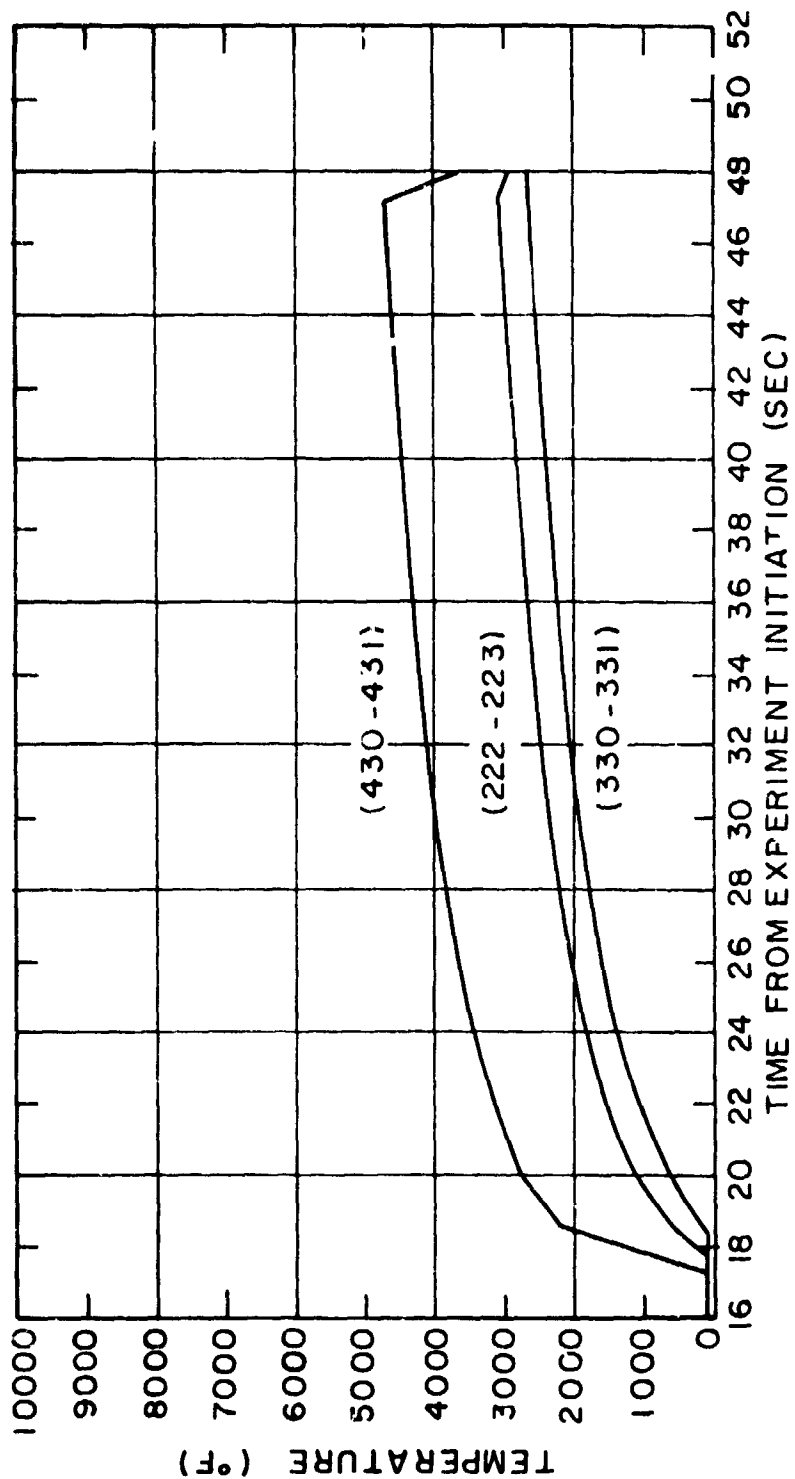
Note: Curves denote the average temperatures of nodes in parentheses and show the temperatures of the upper surface.

FIGURE 11 Calculated Temperature Histories of Points on Weld Circle in Quadrant 2



Note: Curves denote the average temperatures of nodes in parentheses and also show the comparison between temperatures of the upper and the lower surfaces.

FIGURE 12 Calculated Temperature Histories of Points on Weld Circle in Quadrant 3



Note: Curves denote the average temperatures of nodes in parentheses and also show the comparison among temperatures of the upper, the middle, and the lower surfaces.

FIGURE 13 Calculated Temperature Histories at Point where Heat Source Dwells



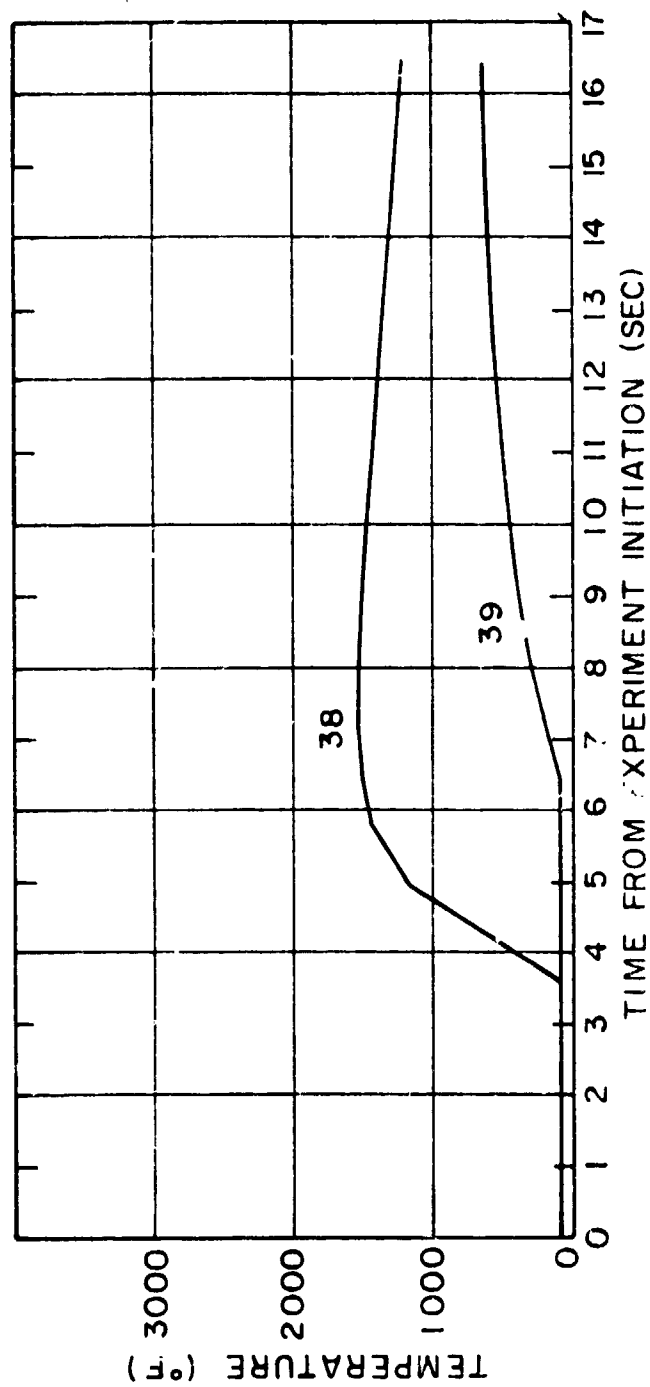


Figure 14 Calculated Temperature Histories of Nodes outside of Weld Circle in Quadrant 1

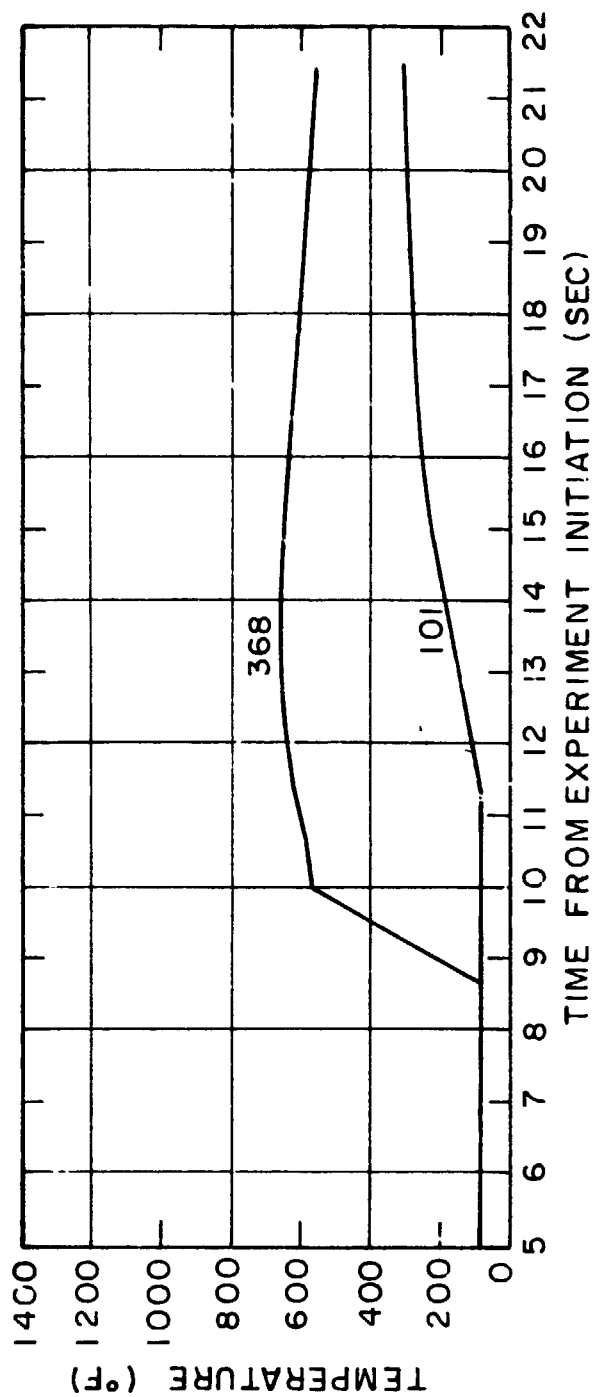
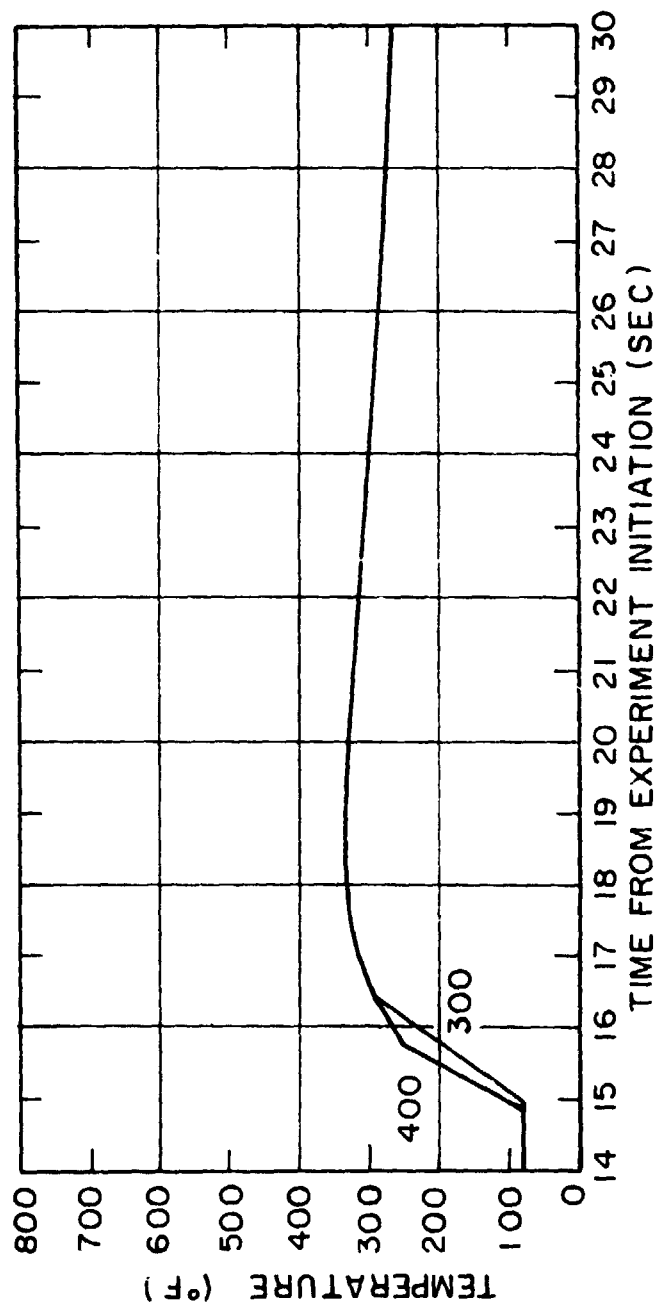
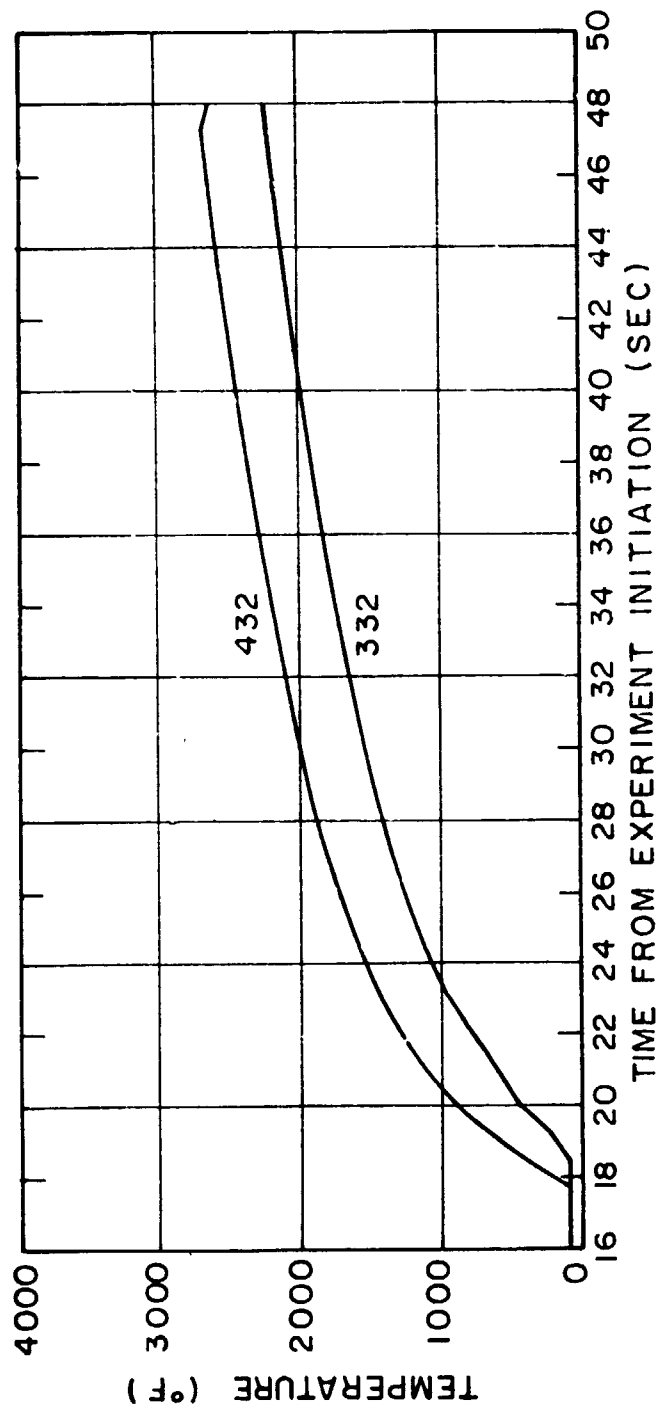


Figure 15 Calculated Temperature Histories of Nodes outside of Weld Circle in Quadrant 2



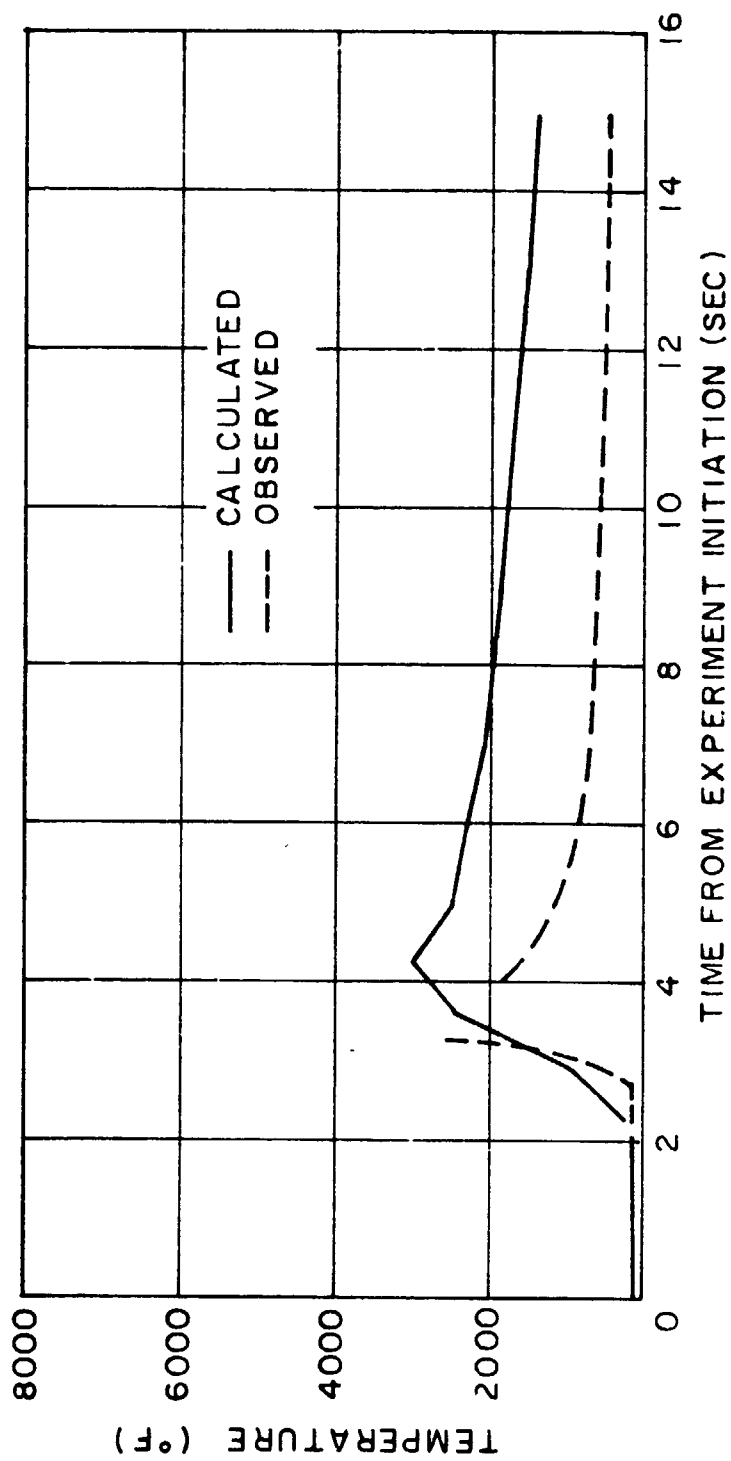
Note: Curves show the comparison between temperatures of the upper and the lower surfaces.

FIGURE 16 Calculated Temperature Histories of Nodes outside of Weld Circle in Quadrant 3



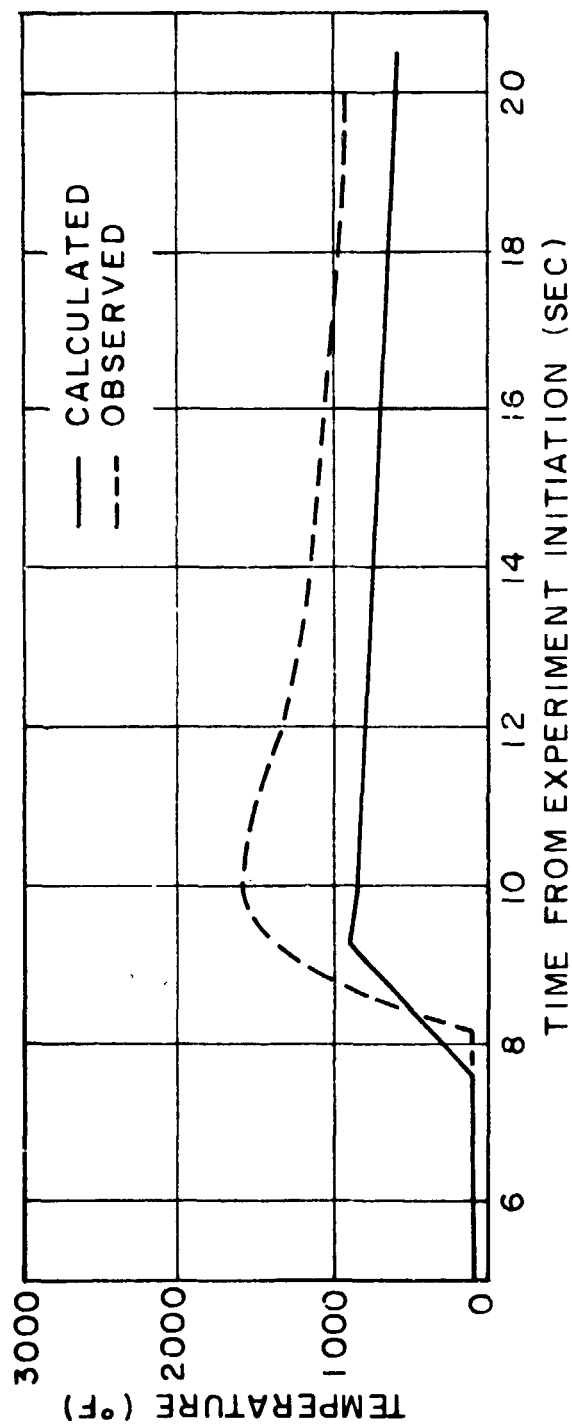
Note: Curves show the comparison between temperatures of the upper and the lower surfaces.

FIGURE 17 Calculated Temperature Histories of Nodes concerning Dwelling Heat Source



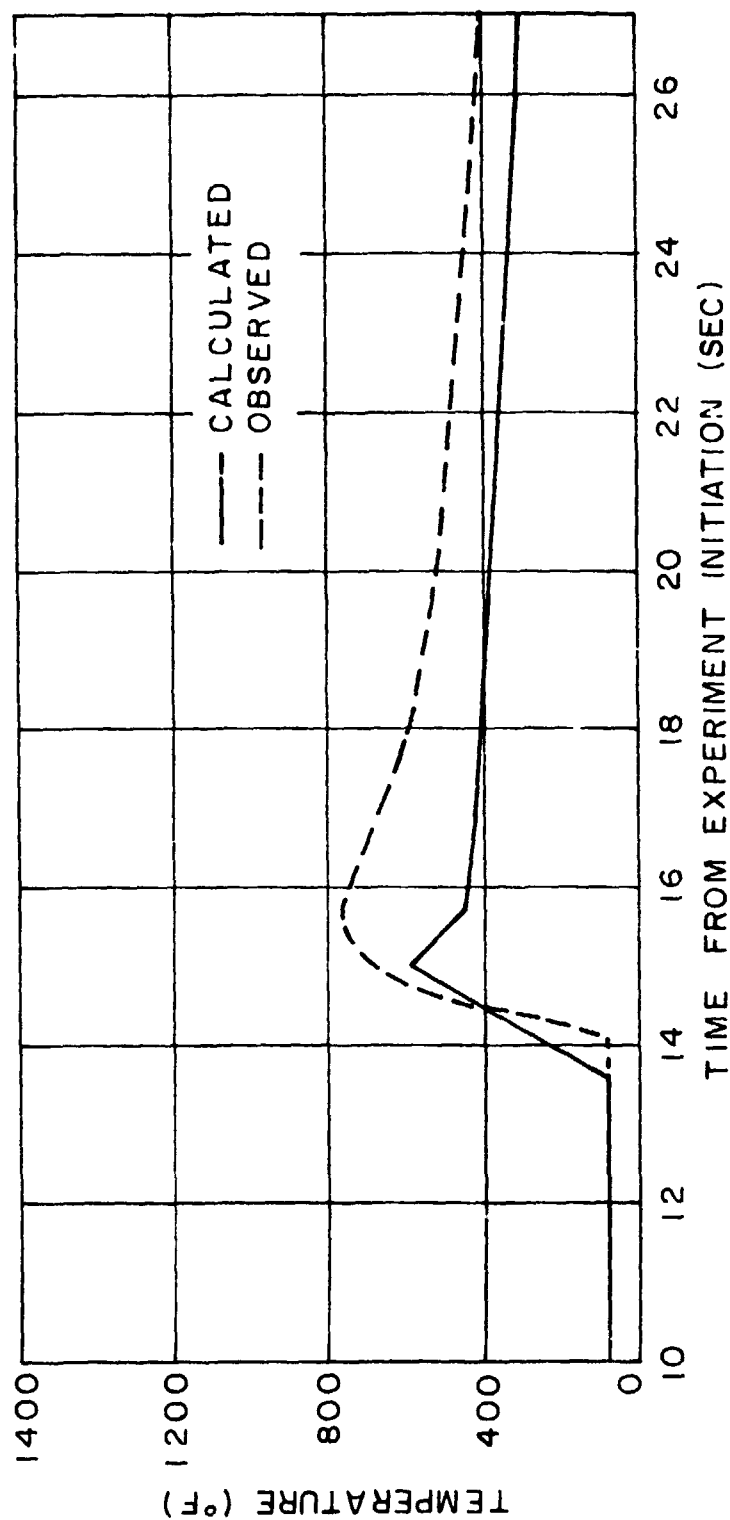
Note: Point is a distance of 2.4 inches from center of disc

Figure 18 Analytical and Experimental Temperature Histories of Points in Quadrant 1



Note: Point at a distance of 2.125 inches from center of disc

Figure 19 Analytical and Experimental Temperature Histories of Points in Quadrant 2

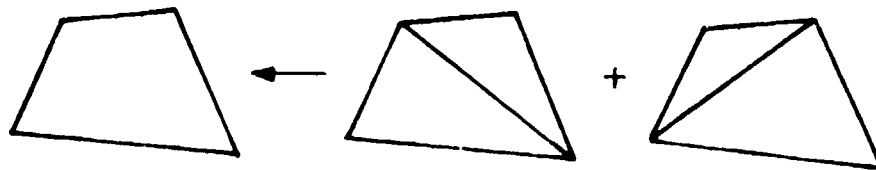


Note: Point at a distance of 2.125 inches from center of disc

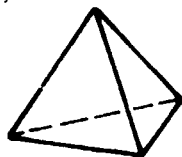
Figure 20 Analytical and Experimental Temperature Histories of Points in Quadrant 3



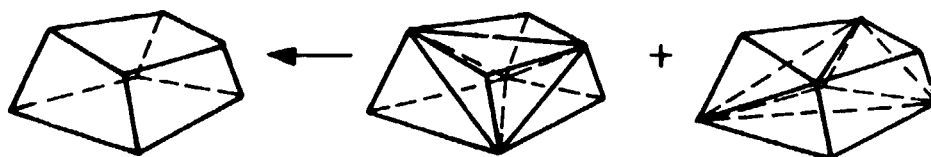
(a) BASIC TRIANGULAR ELEMENT



(b) COMPOSITE ELEMENT



(c) BASIC TETRAHEDRON



(d) COMPOSITE ELEMENT

Figure A-1 Finite Elements Prepared for Analysis



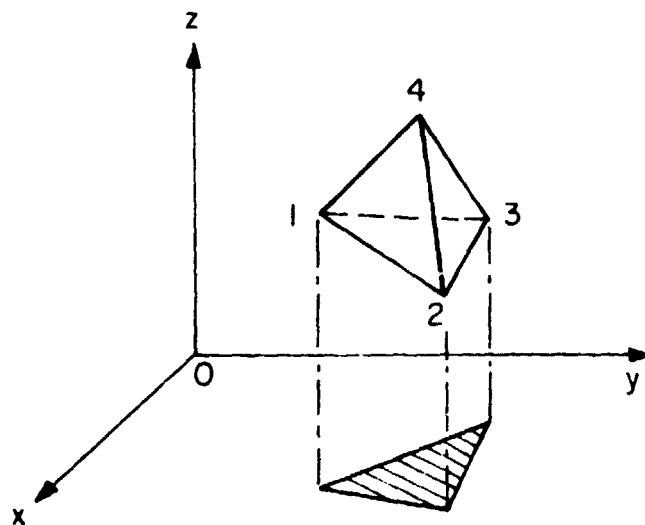
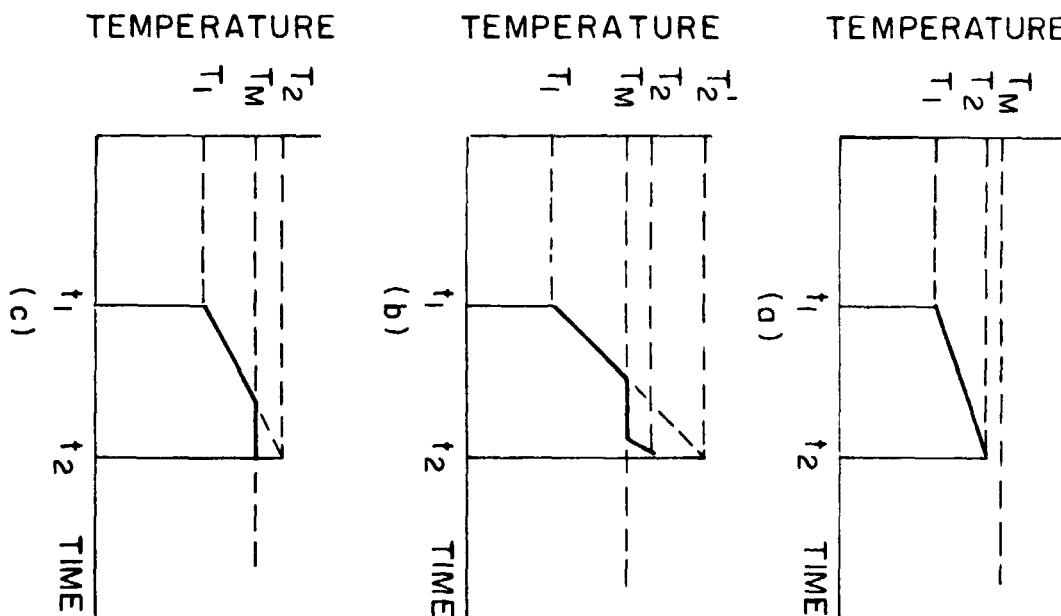


Figure A-2 Basic Three-Dimensional Element and Nodal Times



- Note: (a) Heat is not supplied enough to melt an element.  
 (b) Heat is supplied enough to melt an element.  
 (c) Heat is supplied enough to melt part of an element.

Figure A-3 Models to Consider Metal Melting